SAND79-7088
Unlimited Release
UC-94b Distribution

Conceptual Design of a Flywheel Energy Storage System Final Report

William M. Brobeck & Associates

Prepared by Sandia Laboratories, Albuquerque, New Mexico 87185 and Livermore, California 94550 for the United States Department of Energy under Contract DE-AC04-76DP00789

Printed December 1979

Prepared for Sandia Laboratories under Contract No. 07-3

Sandia Laboratories

SF 2900 Q(7-73)

Issued by Sandia Laboratories, operated for the United States Department of Energy by Sandia Corporation.

Printed in the United States of America

Available from
National Technical Information Service
U. S. Department of Commerce
5285 Port Royal Road
Springfield, VA 22161

Price: Printed Copy $6.50; Microfiche $3.00

DISCLAIMER NOTICE

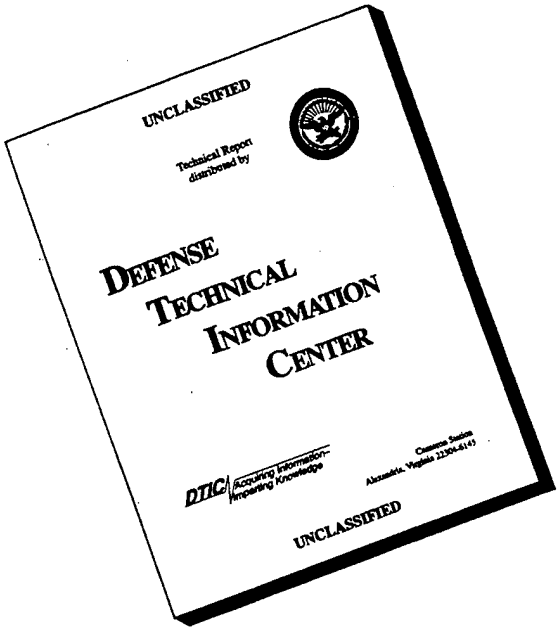

THIS DOCUMENT IS BEST QUALITY AVAILABLE. THE COPY FURNISHED TO DTIC CONTAINED A SIGNIFICANT NUMBER OF PAGES WHICH DO NOT REPRODUCE LEGIBLY.

SAND79-7088
Unlimited Release
Printed November 1979

Distribution
Category UC-94b

CONCEPTUAL DESIGN
OF A
FLYWHEEL ENERGY STORAGE SYSTEM

FINAL REPORT

SANDIA CONTRACT NO. 07-3663

Prepared for

SANDIA LABORATORIES
Albuquerque, New Mexico

Contract Technical Monitor
Harold Schildknecht, Division 2324

Prepared by

WILLIAM M. BROBECK & ASSOCIATES
1235 Tenth Street
Berkeley, California 94710

Report No. 4500-92-9-R1

APPROVALS

Issue	Contents	Prepared by	Approved by
Original	viii + 92 pages	William H. Bauer Hayden S. Gordon Gregory V. Hassman Stephen F. Post Francis C. Younger	Francis C. Younger Project Director

Checked By

Stephen F. Post

FOREWORD

This report represents the results of a conceptual design study carried out by William M. Brobeck and Associates (WMB&A) for Sandia Laboratories under Sandia Contract No. 07-3663. Mr. Harold E. Schildknecht is the Sandia Contract Technical Monitor, and his cooperation and guidance are gratefully acknowledged. The effort was reviewed at its midpoint at the U.S. Department of Energy, Division of Energy Storage System with the Branch Chief for Advanced Physical Methods, Dr. George C. Chang. His helpful suggestions and continuing interest in this program are gratefully acknowledged.

The work described in this report was carried out under the direction of WMB&A Project Director, Mr. Francis C. Younger. Messrs. Stephen F. Post and William H. Bauer have assisted in formulation of approaches, review of conclusions and have carried out many of the design analyses. Messrs. Gregory V. Hassman and Robert E. Thomas have carried out much of the control circuit analyses and aided greatly in the motor selection study. Dr. Hayden S. Gordon has provided valuable assistance in economic analysis and cost estimating.

The design concept presented in this report should be considered conceptual. Minor changes in the design may be anticipated in a continuation from a conceptual design toward a prototype design. It is hoped that such a continuation would proceed in stages which would include fabrication and testing of a demonstration unit.

TABLE OF CONTENTS

LIST OF FIGURES

LIST OF TABLES

ABSTRACT

A conceptual design of a flywheel energy storage system suitable for on-site interfacing with residential photovoltaic (PV) energy sources has been developed. The basic design objective was to provide a generous margin of safety and above average reliability and efficiency at the lowest practical cost. This report describes the basic design concept and the general approach to the conceptual design of the energy storage system. The basic concept to interface with PV energy sources utilizes a constant voltage motor/generator directly coupled to a flywheel rotor. The voltage level of the motor is maintained at the optimum operating voltage of the array of PV cells and permits peak power tracking. Power is withdrawn from the flywheel-driven generator when the voltage output of the array drops below its optimum value, and power is delivered to the flywheel via the generator (then operating as a motor) when the voltage rises above the optimum value. A variety of motor types and flywheel rotor types has been studied to arrive at a conceptual design to meet the program objectives. A fiber-composite rotor driving a separately-excited motor satisfies the basic requirements. To obtain acceptable efficiency and low run-down losses, the flywheel operates in a vacuum and has a combination of magnetic thrust support and ball bearings to reduce bearing friction in an economical fashion. The need for rotary vacuum seal is eliminated by the use of a hermetically-sealed magnetic power coupling.

Cost of the system has been determined for production models to be produced in annual quantities up to one-hundred thousand for both ten-kWh and fifty-kWh capacities, and also for a ten-kWh one-of-a-kind demonstration model.

INTRODUCTION

The Flywheel Energy Storage System (FESS) is intended to enhance the value and utility of small solar power generating plants. The timely development of economical energy storage concepts is crucial in many solar power applications. The variable nature of solar energy severely limits its applications if some practical storage system is not made available. Batteries, pumped-hydro, compressed air, thermal and mechanical energy storage all offer the potential for suitable systems applications. Economic factors may favor one system in a particular application and yet another in a different application depending upon their performance and cost characteristics. However, at present, accurate cost and performance characteristics do not exist for emerging technologies. New designs with generous margins of safety have not yet been demonstrated for mechanical energy storage systems. A concept which could lead toward a practical demonstration is presented.

This report describes the effort for the development of a conceptual design for a FESS suitable for on-site interfacing with small photovoltaic (PV) energy sources. The new design has as objectives a generous margin of safety, high reliability and efficiency obtained at the lowest practical cost. The design is for a stationary application, in which volume and weight are of secondary importance. The basic design objective is a system which can be economically manufactured in existing industrial facilities using conventional production methods.

Attainment of the highest practical charge/discharge efficiency is a high priority goal. This requires very careful attention to design details, as well as the selection of the most appropriate engineering concept.

The program objective is the design of storage units suitable for use with small to intermediate scale solar sources. The nominal energy storage capacity is in the range of 5 kWh to 100 kWh; the specific requirements are for the detailed design of a 10-kWh storage system and for detailed cost estimates of the 10-kWh system and a 50-kWh system. The required power rating of the 10-kWh system is 5 kW. These units are to have an electrical interface for 60 Hz/220 volts single-phase power. The control system must maintain the desired frequency and voltage over the full rotor operating speed range.

The round-trip efficiency for charging and discharging must exceed 70 percent. This requires that the one-way efficiency exceed 84 percent. The rate of loss of stored energy due to friction and windage must not exceed five percent per hour.

The design must have a generous factor of safety and high reliability. It must be designed for a life expectancy of at least twenty years during which a minimum of 10,000 charge/discharge cycles may be encountered. These cycles cover the full speed range of the design. Allowance may have to be made for any overspeed tests which might occasionally be performed.

The project is divided into four main tasks covering (1) the basic system concept; (2) optimization; (3) design of a 10-kWh unit; and (4) estimate for a 50-kWh unit.

The basic system concept effort and subsystem options consist of an evaluation of workable engineering concepts and the narrowing down of choices to the best subsystem options. Subsystem options include flywheel configuration, materials, flywheel housing and containment, seals, type of motor/generator, suspension system, mounting, controls, auxiliaries, and instrumentation. Problems of safety, efficiency, losses and parasitic loads, manufacturability, maintenance, and economics are considered.

Various flywheel configurations and material combinations have been considered for energy storage systems. It has been shown that high energy density is achievable with materials possessing a high strength-to-weight ratio, and that some of these materials are sufficiently inexpensive to be potentially attractive for residential use.

The results of the design study may be summarized as follows:

1. A conceptual design satisfying the program objectives has emerged.
2. The study shows that a rim-type flywheel using filament-wound fiber composite based on E-glass/epoxy is the most economical flywheel for a FESS.
3. The projected rotor cost for the 50-kWh FESS is $198 per kWh of stored energy.
4. Peak power tracking for the PV supply is easily accomplished for the FESS.
5. A separately excited motor/generator with transistorized electronics commutation can provide mechanical to electrical energy conversion with high turn-around efficiency.

6. Low windage losses for the flywheel will require maintaining a vacuum of about 2×10^{-7} atmospheres.

7. To assure low bearing friction partial support of the flywheel weight using a magnetic thrust bearing is required.

8. By coupling power magnetically across a non-conducting vacuum barrier the need for a rotating seal is eliminated.

9. High reliability and safety appears achievable.

10. A total system cost of about $371 per kWh of deliverable energy appears possible for large production.

11. A ten-kWh demonstration model can probably be produced for about $207,000 not including testing, administration and further design.

From the results of the design study it can be concluded that a FESS would be practical in some regions if the unit is properly sized to take advantage of the available energy at the particular site. The optimum size may be about 25 kWh depending upon the size of the PV supply. It may also be concluded that a demonstration model can be fabricated using presently available technology.

TEN-kWh SYSTEM DESCRIPTION

CONCEPT

The FESS concept integrated with a residential photovoltaic (PV) supply is shown in Figure 1. The FESS acts as an energy buffer between the direct current PV supply and the alternating current utility power source to permit an optimum utilization of the available solar energy. The PV supply represents a variable voltage dc source with its voltage dependent upon its temperature and current and upon the solar insolation. With increasing insolation, the available PV energy will rise and may exceed the load demand of the home; excess power is then diverted for storage in the flywheel shown in the pit below the garage floor. This stored energy is subsequently recovered to supply electrical energy to the home when the available solar energy is inadequate to satisfy the demand.

In addition to providing an energy storage capacity via the flywheel, the FESS provides the necessary energy conversions to match the requirements of the various portions of the integrated system. These include the conversions from mechanical (kinetic) energy to electrical energy, from dc to ac, and the tracking of optimum dc voltages. Figure 2 shows the general flow of power and main system elements. The generator coupled to the flywheel provides the electrical to mechanical energy conversion using adjustable field current to provide control of the power flow. The generator converts mechanical energy into electrical energy to discharge the flywheel when there is a demand for its energy or it acts as a motor to reverse the energy flow when there is a surplus of solar energy.

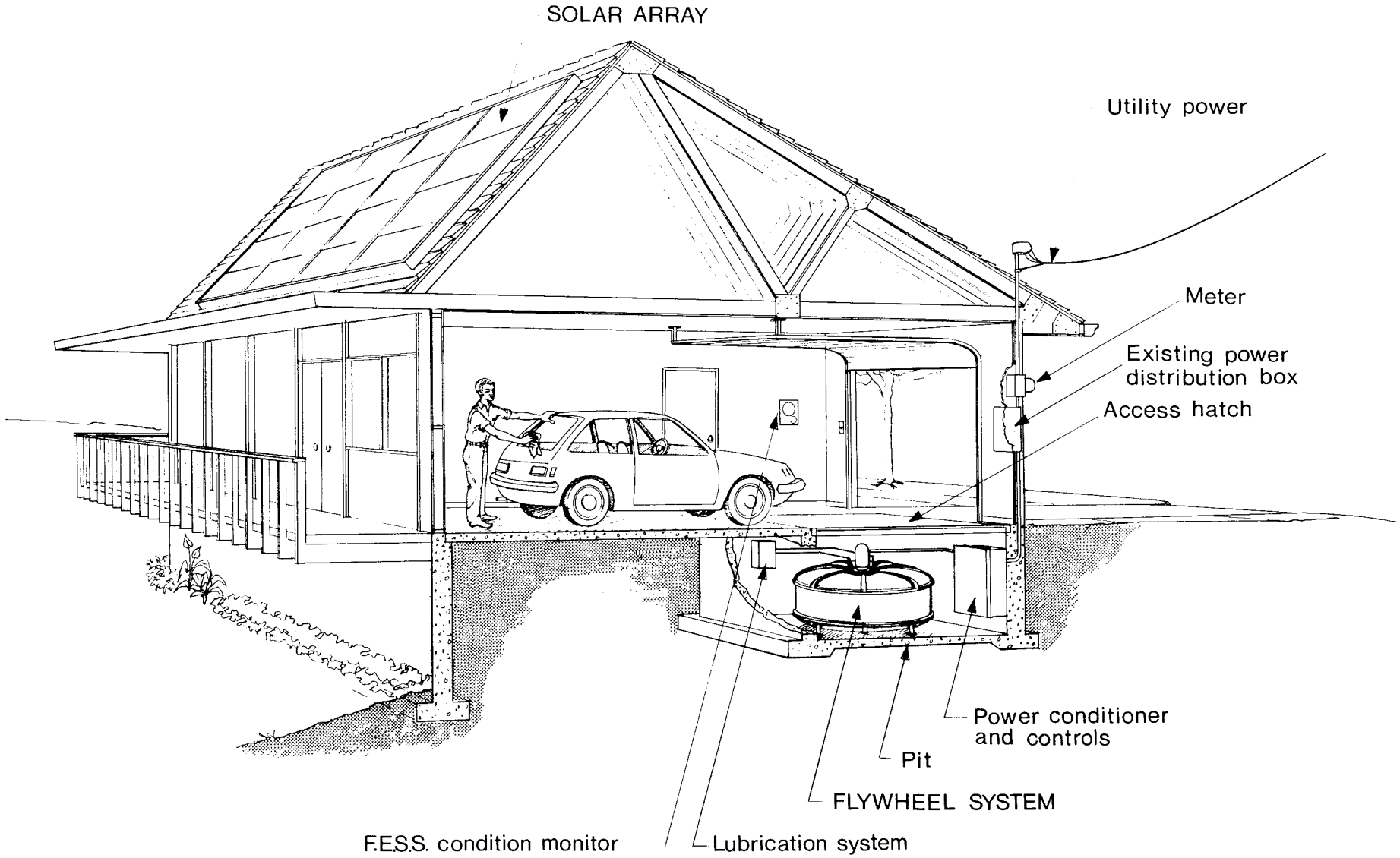

Figure 1. Residential Flywheel Energy Storage System

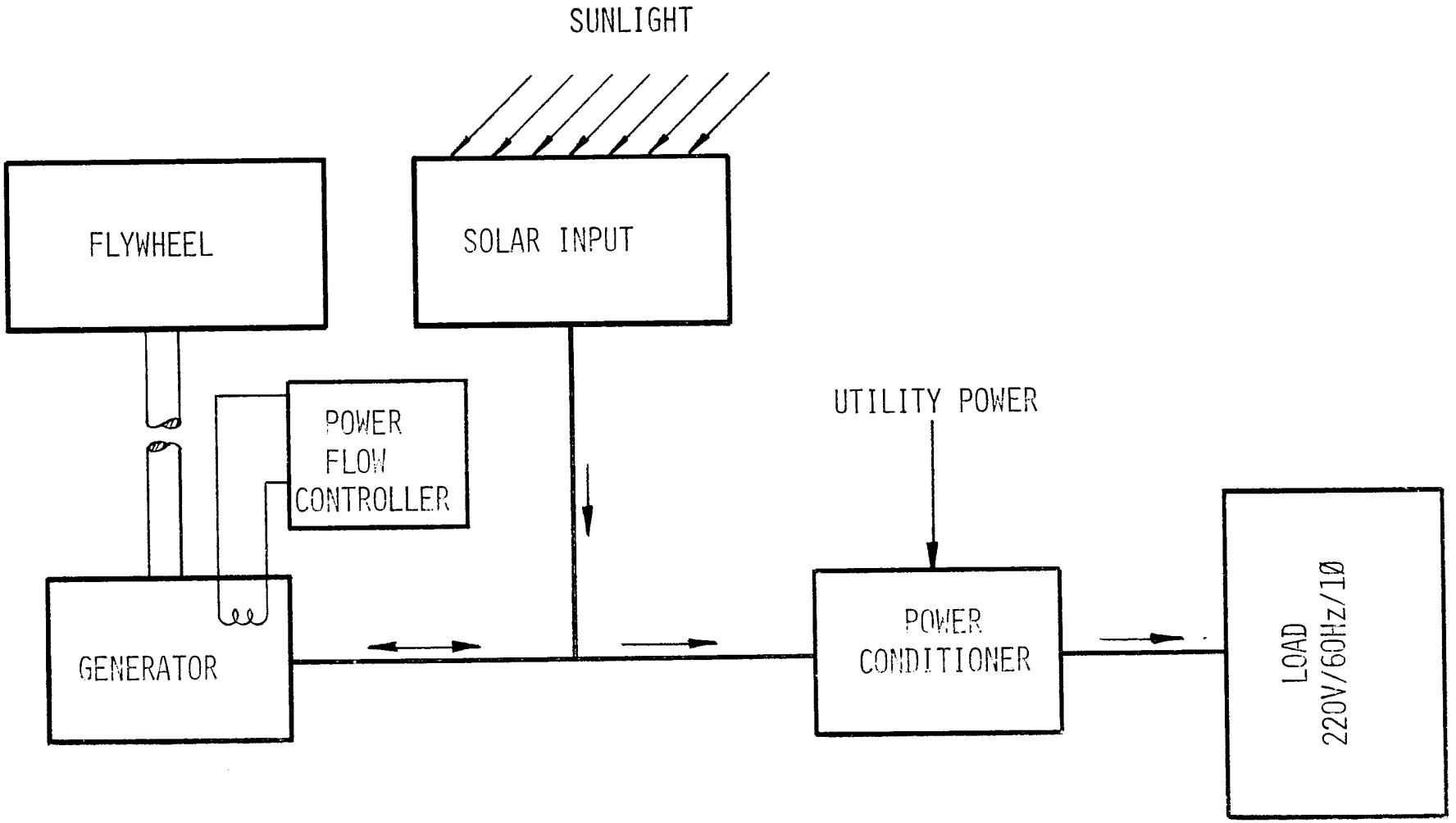

Figure 2. Power Flow Schematic for FESS

The link shown between the solar unit, the generator, and the power conditioner is a dc link set at the voltage which optimizes the power output of the PV cells. This optimum value of voltage depends upon the temperature of the PV cells and the solar insolation. The voltage is controlled by the field excitation of the generator and the flywheel speed. As the flywheel speed increases, the field current is reduced to maintain the desired voltage. The power conditioner provides the required dc to ac conversion.

The flywheel/generator system is shown in Figures 3 and 4. The main elements are the flywheel, motor/generator, vacuum vessel and the flywheel suspension system. The suspension system consists of support bearings to carry the flywheel weight and dynamic loads and damper assemblies to prevent whirl instabilities.

The FESS design concept was developed specifically for a 10-kWh storage capacity system with a 5-kW maximum power output. However, special emphasis was placed on assuring that the concept was adaptable for upward scaling to 50-kWh storage capacity and 10-kW maximum power output. Table 1 provides a comparative listing of the design features that primarily serve to distinguish the 10-kWh and 50-kWh storage capacity configurations.

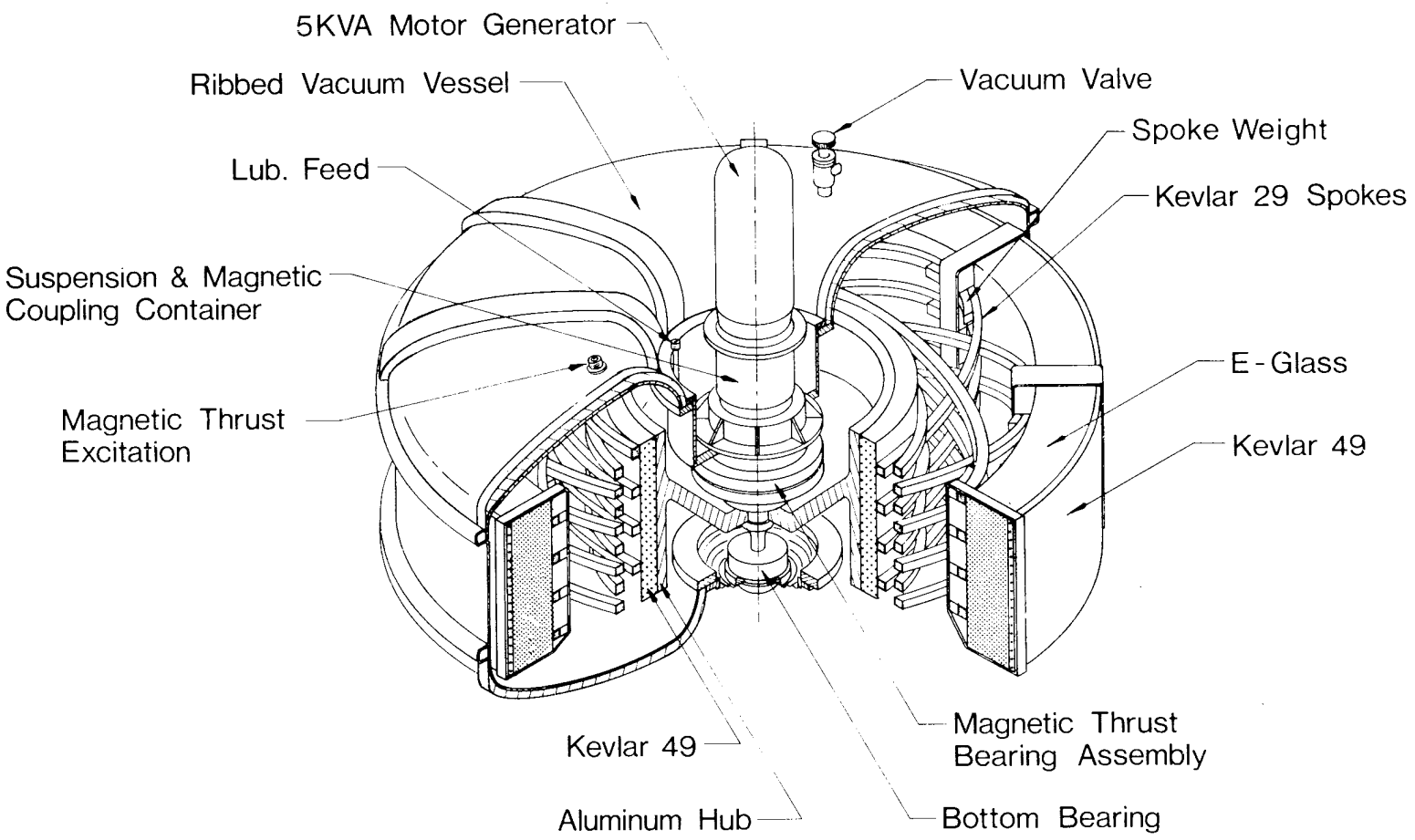

Figure 3. Ten-kWh FESS Cut-Away View

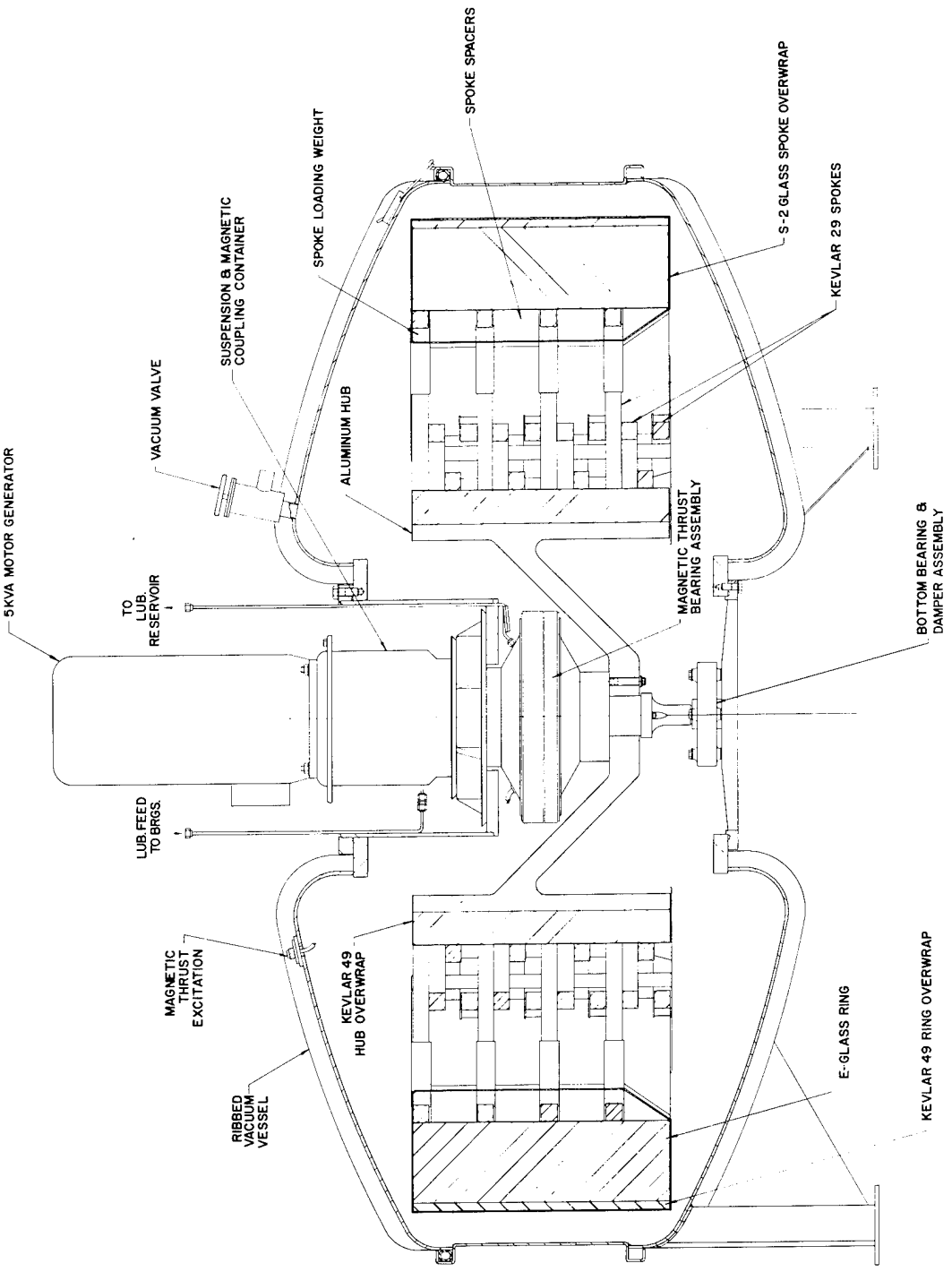

Figure 4. Ten-kWh FESS Cross-Section

Table 1. FESS Design Features

	10 kWh	50 kWh
Working Speed, rpm		
Maximum	9800	5730
Minimum	4900	2860
Rotor Characteristics		
Outside Diameter, in	49.88	85.29
Inside Diameter, in	40.88	69.90
Height, in	13.12	22.43
Weight, lb	906	4530
Maximum Energy Density, Wh/lb	14.9	14.9

A foremost objective of the contractual scope of work was to develop the conceptual design of a low-cost conventionally manufacturable 10-kWh FESS. Hence, this section places primary emphasis on the description of a production-model version of the basic 10-kWh design concept shown in Figure 3.

A 10-kWh concept as embodied in a one-of-a-kind demonstration model and the aforementioned 50-kWh system in a production-model configuration are described in subsequent sections, although most of the design features of the production-model 10-kWh FESS are common to the demonstration model and the 50-kWh system.

MECHANICAL DESIGN

Ten-kWh Rotor

The rotor as shown in Figure 5 is a biannulate rim supported by tension-balanced polar-catenary spokes which connect the central hub and the rim. For the 10-kWh unit, the biannulate rim, consisting of a fairly thick portion filament wound with E-glass/epoxy and a thin circumferential overwrap of Kevlar 49/epoxy, has an outside diameter of 1.267 m (49.88 in) and an inside diameter of 1.038 m (40.88). The glass/Kevlar interface diameter is 1.249 m (49.16 in). The rim axial length is 333 mm (13.12 in). The relatively large amount of the inexpensive E-glass keeps the cost down and the high modulus Kevlar 49 overwrap suppresses the radial tension stresses which otherwise would occur in a thick rim. This design permits a high volumetric energy density since a large percent of the swept volume of the flywheel is occupied by highly stressed fiber-composite material. The rim weight is 278 kg (613 lbs) and the total weight is 411 kg (906 lbs). For 10-kWh of available energy, the peak stored energy is 13.5 kWh at 9800 rpm, and the energy density is 32.8 Wh/kg (14.9 Wh/lb).

A 584-mm (23-in) diameter hub reduces the radial space between the hub and rim to allow the Kevlar 29 spokes to be short enough to provide adequate rigidity to maintain hub/rim concentricity.

The rotor assembly incorporates sixteen spoke loops, with each loop providing four spokes for a total of 64 spokes. Each spoke is .89 inch thick by .82 inch wide. The contour of the spokes is a polar catenary, the natural shape of a flexible cord in a centrifugal force field. This contour theoretically eliminates all bending moments in the spokes, and helps to reduce the maximum stress to a moderate level.[1]

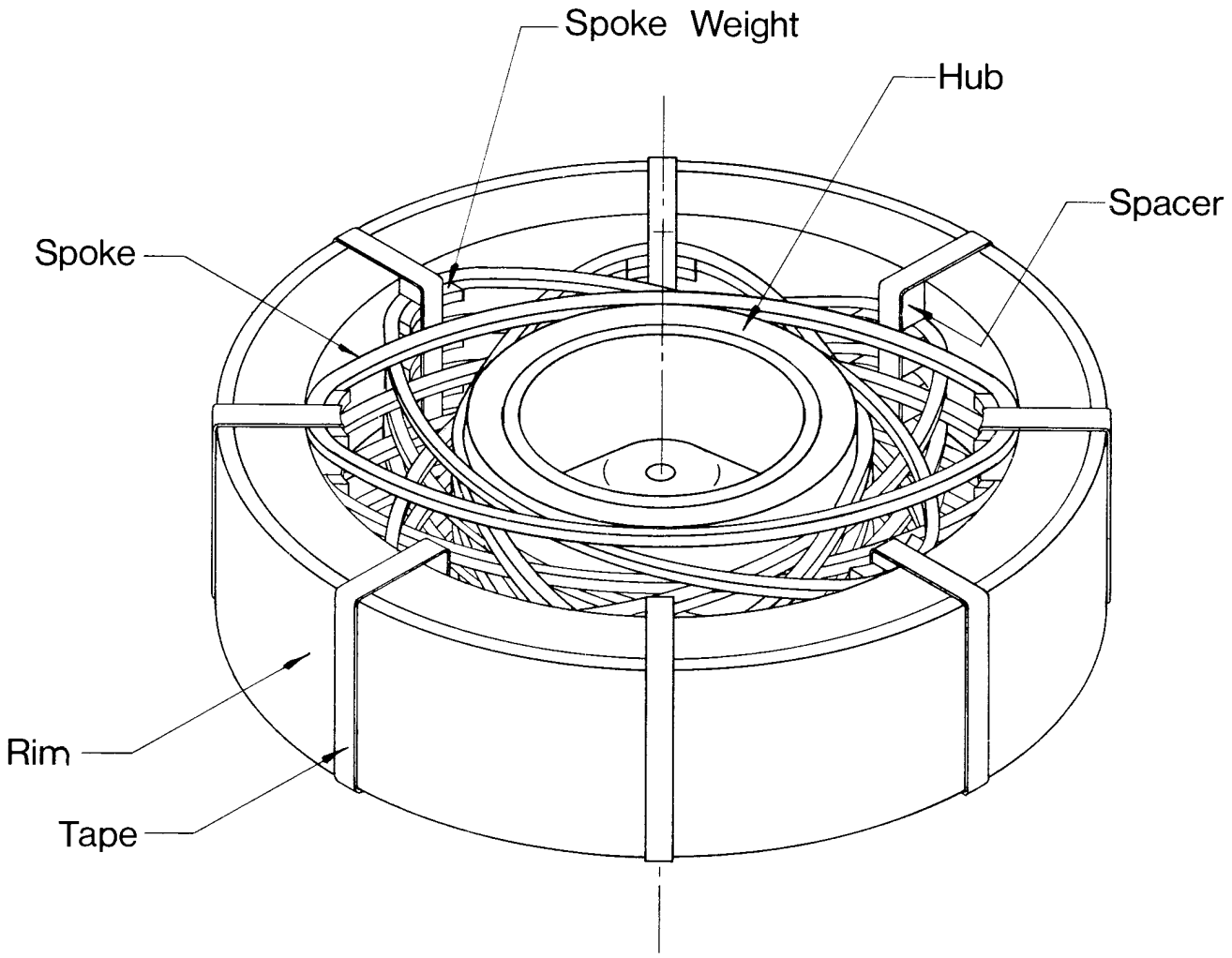

Figure 5. Biannulate Rim Flywheel

The spokes contain steel loading weights at the junction with the rim. The centrifugal force on these weights causes the spokes to expand radially. The weights are sized to produce an expansion to match that of the rim thereby virtually eliminating radial loading on the rim. The low modulus of elasticity of the Kevlar 29 allows the loading weights to be small enough to minimize spoke tension stresses. There are a total of 32 weights (i.e. two per spoke loop) and each weighs 1.7 pounds.

The hub is made from aluminum alloy and is strengthened by a pre-stressed Kevlar 49 overwrap which partially resists the centrifugal loading on the aluminum portion. The radial stresses in the hub are minimized by its conical shape. The overwraps fit onto the aluminum with a diametral interference of .013 inches to produce a compressive preload which acts to reduce the maximum tensile stress in the aluminum caused by centrifugal loading.

A section view of the hub was shown in Figure 4. The conical shape of the center web allows the hub rim to dilate under centrifugal loading without creating excessive stress in the web.

Suspension System

The suspension system consists of a combination of precision ball bearings and a magnetic thrust bearing as shown in Figures 6 and 7. The magnetic thrust bearing supports 90 percent of the rotor weight and is shown as two parts. The upper part labeled "wound lifting mag.(stationary)" is the portion that is electrically energized to attract the lower part labeled "lifting mag. (rotating)." Both parts are silicon iron with an outside diameter of 273 mm (10.75 inches) and the gap between these two

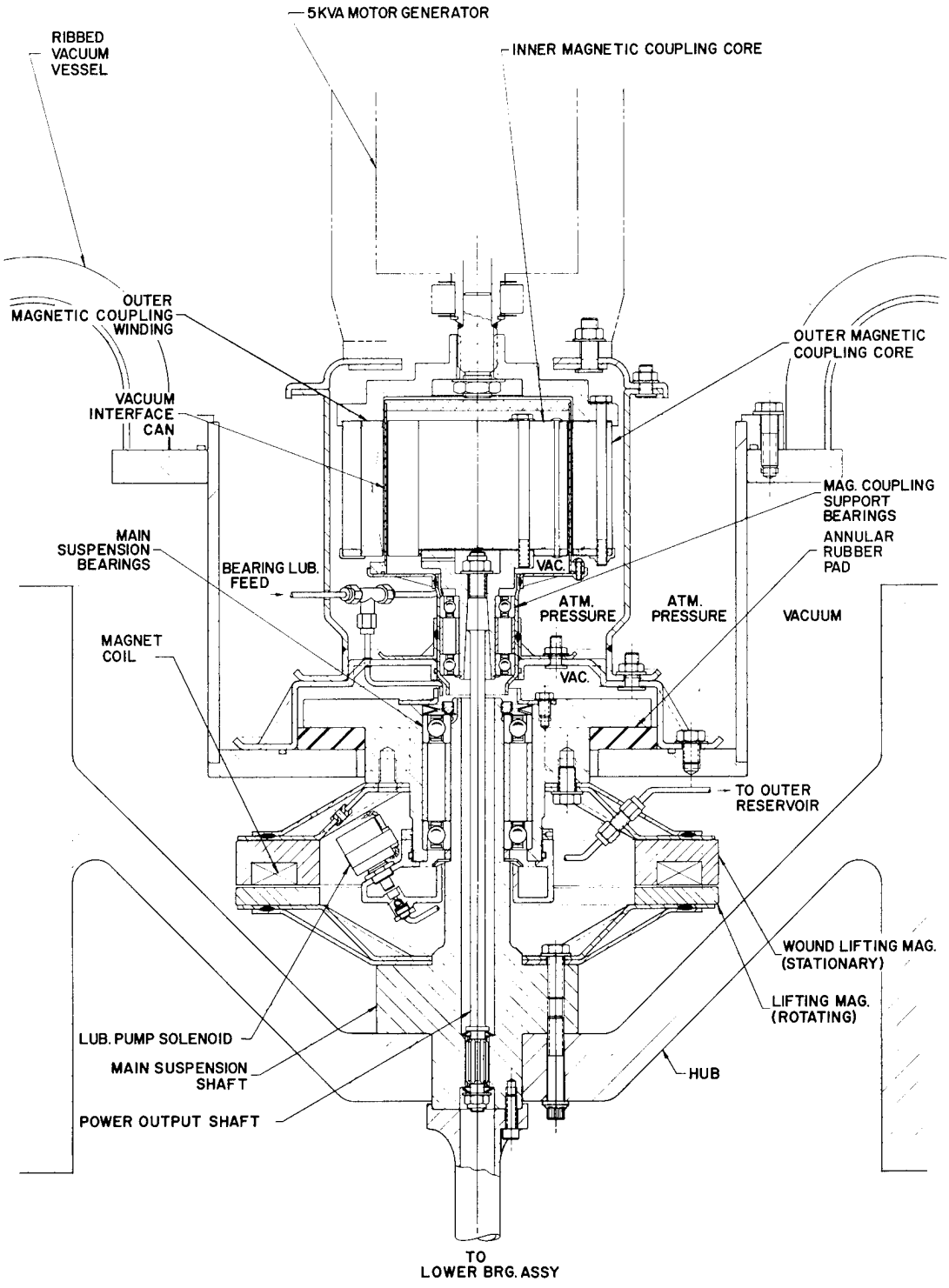

Figure 6. Ten-kWh FESS Suspension and Magnetic Coupling

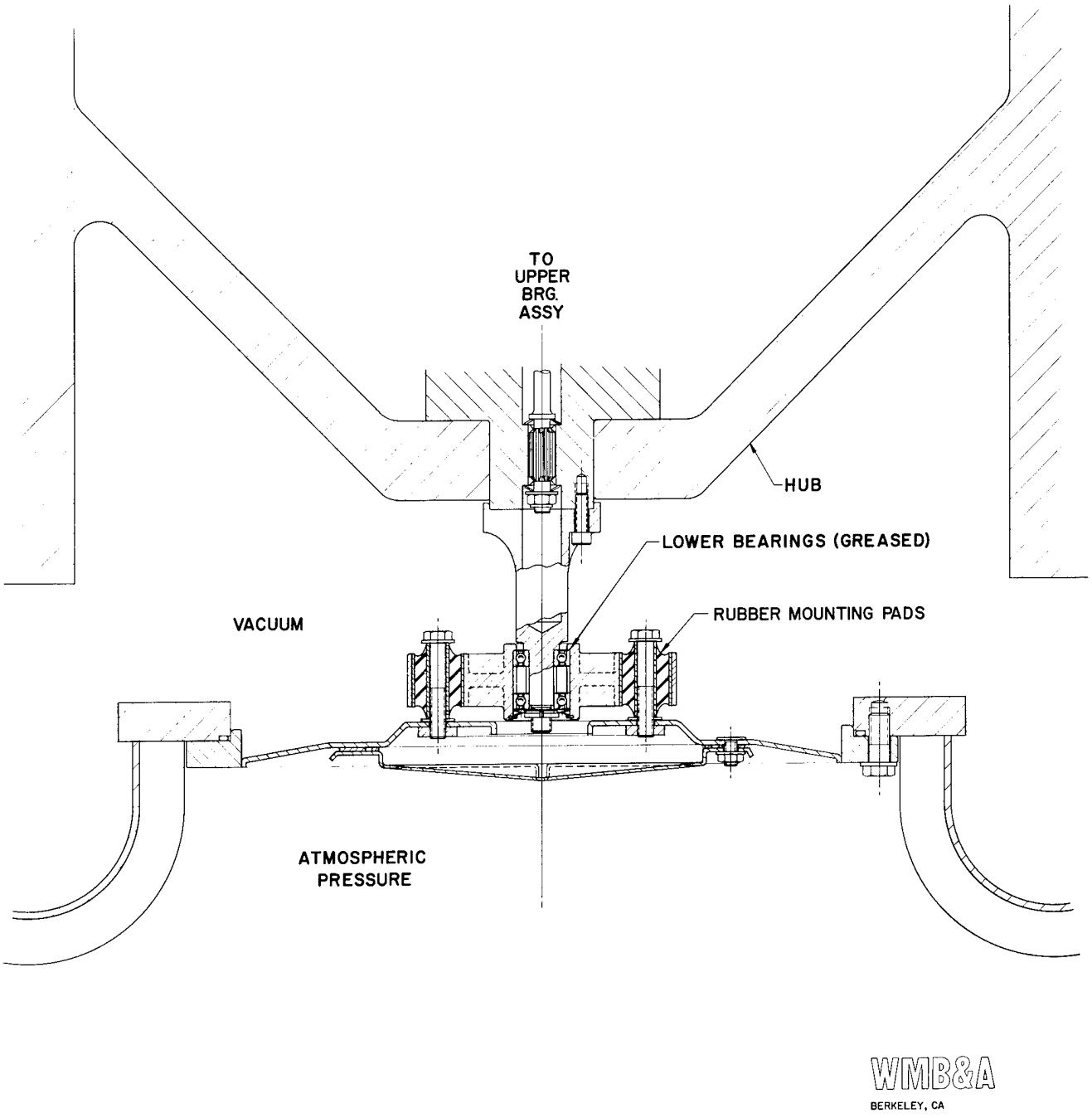

Figure 7. Ten-kWh FESS Lower Suspension

parts remain constant even if the rotor is experiencing a small precession with nutation.

The precision ball bearings maintain the required radial alignment of the rotor relative to the drive motor and support ten percent of the rotor weight. The housing for the main suspension bearings is attached to the vacuum vessel through an annular rubber pad. The resiliency of this pad permits a limited amount of radial motion of the rotor to accommodate a small amount of rotor unbalance without imposing excessive radial loads on the bearings. A small amount of precessional motion is also permitted. The lower bearing support shown in Figure 7 is also mounted in rubber to permit a limited amount of motion. The rubber mounting pads provide damping to prevent dynamic instability. The system operates above the critical speed where asynchronous whirl modes can be excited unless adequate damping is provided.[2]

The upper bearings are lubricated by an oil drop system. Oil is injected into the top of the housing one drop at a time. The drop turns into mist as it hits the high speed rotating parts. Surplus oil is collected in a reservoir below the housing. A small solenoid-powered plunger intermittently pumps this oil to an evacuated exterior reservoir, from which it again flows to the top of the housing to repeat the cycle. Because of their light loading the lower bearings can be lubricated with grease.

Power Output Shaft

The power output shaft must be flexible enough to accommodate the precessional motion of the rotor. To achieve the desired flexibility requires the use of a comparatively small diameter (.5 inch) "quill" shaft of

substantial free length (7.8 inch) as shown in Figure 6. This shaft is made from heat treated steel with adequate strength and toughness to assure that its deflections are entirely in the elastic region. The quill shaft presents a special design problem in that its flexibility has upper and low limits. Excessive stiffness will lead to failure via excessive stress. Inadequate stiffness will allow shaft whip.[3] Although this is a sensitive design area, simultaneously satisfying both requirements is usually not too difficut.

Magnetic Coupling

The purpose of the magnetic coupling is to transfer torque through the vacuum vessel without the use of a dynamic seal. The coupling is illustrated in Figure 8. Both the inner and outer cores are constructed from laminated transformer silicon steel. The outer portion of the coupling is driven by the motor and holds the magnet coil windings. The inner portion which is coupled to the flywheel via a 12.7-mm (.5-in) diameter quill shaft is driven synchronously as a salient-pole machine running on reluctance torque. The gap between the inner and outer portion is occupied by a vacuum barrier shown as a "vacuum interface can."

The cylindrical wall of the can is made from G-10, an epoxy composite, 4.12-inch diameter by .03-inch thick in the ten-kWh system.

A plan view of the magnetic coupling assembly is shown in Figure 9. The assembly is three inches long with an outside diameter of six inches.

In order to reduce run-down losses, the coupling is electrically activated only during charging or discharging. The amount of excitation current is a function of the torque transmitted. After a brief start-up

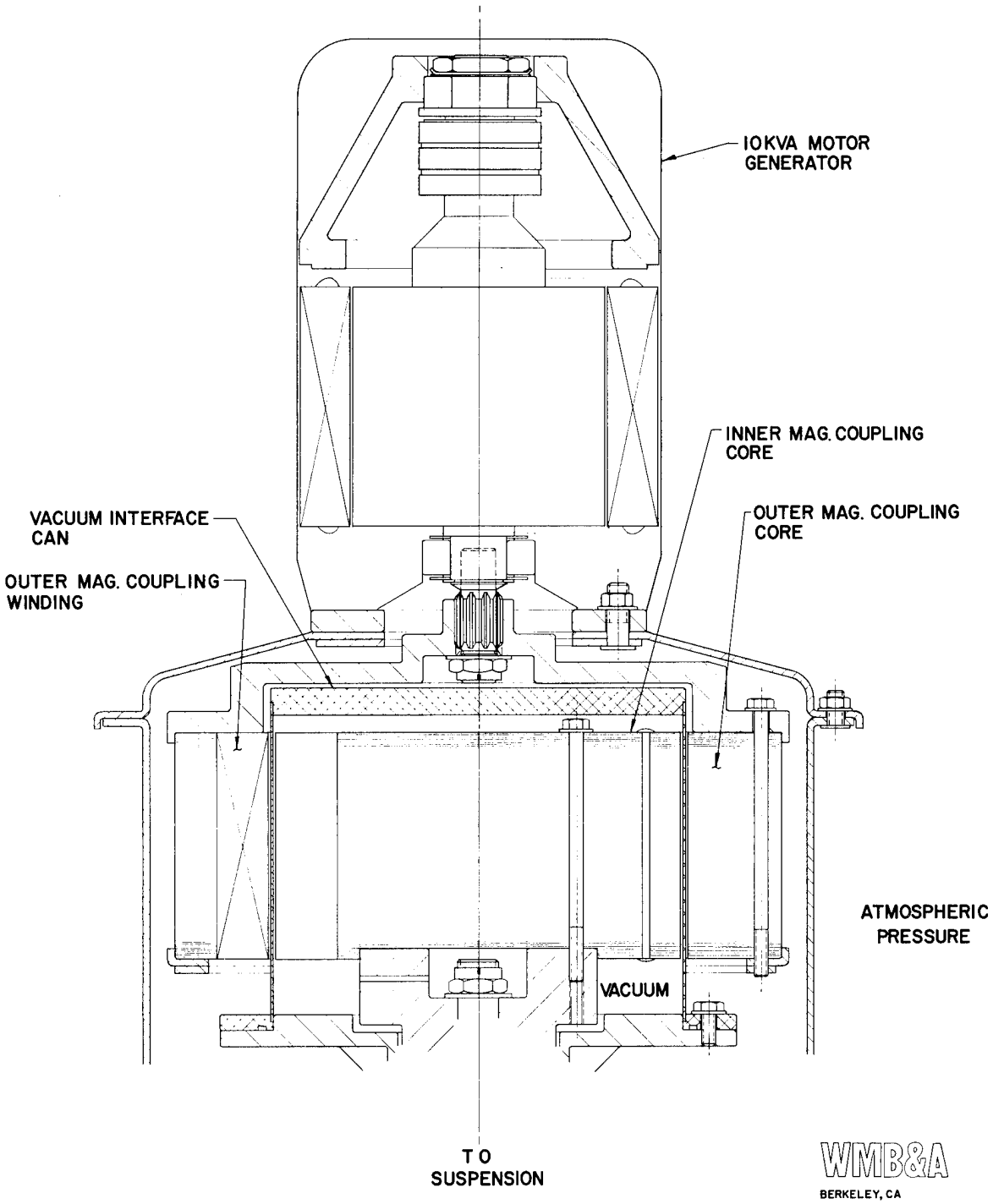

Figure 8. Motor/Generator and Magnetic Coupling

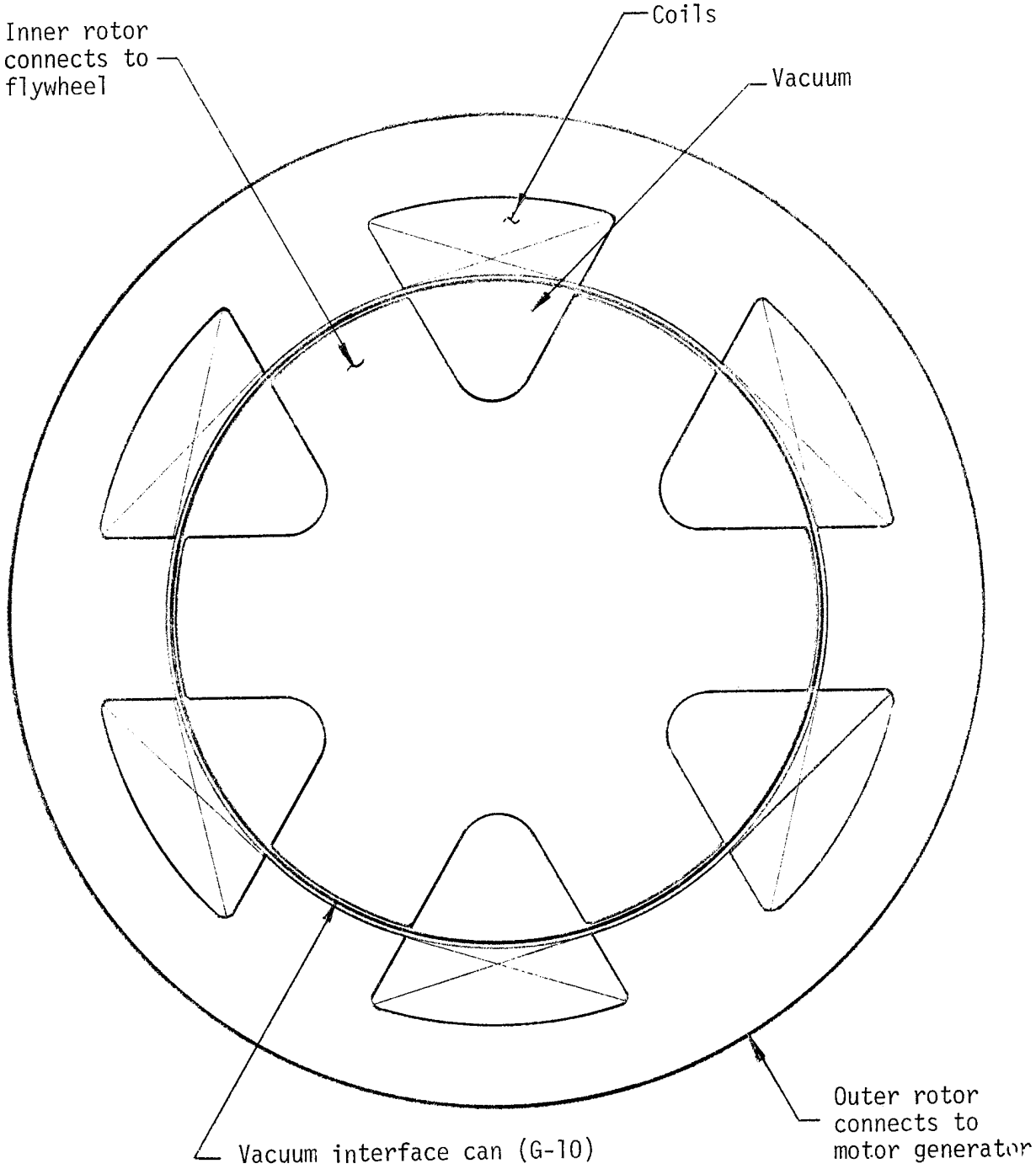

Figure 9. Magnetic Coupling Plan View

period involving slippage the magnetic coupling keeps the rotor and the motor/generator fully synchronized.

Motor/Generator

The motor/generator unit is an air-cooled, separately-excited, three-phase alternator. The unit proposed for the prototype is a modified Bendix 9kVA aircraft alternator designed for high speed use as shown in Figure 10. The required modifications include adding a third slip ring and brush assembly for the magnetic coupling and the removal of the dc exciter section. Figure 11 shows the outline of the modified motor generator. The motor/generator for the production FESS would be a custom-built unit of similar design.

Vacuum Vessel

The vacuum vessel shown in Figure 4 is made from 12 gage (.105 inch) steel stampings. Ribs are used to provide the required rigidity against the vacuum load and to provide adequate bearing support.

An O-ring seal is used to keep vacuum integrity. A valve provides a connection for a vacuum pump for periodic pump down. When the FESS is first assembled and pumped down an initial outgassing period will be encountered. Baking out the system will speed up this outgassing process.[6] Once properly outgassed, the closed system is expected to remain at a sufficiently low pressure for many months, as the epoxy resin has a negligible vapor pressure.[7]

ELECTRICAL DESIGN

Control System Concept

The FESS control system maintains the optimum flow of power from the PV supply by diverting excess power from the PV supply to the flywheel when the available solar power exceed the demand of the home and by taking

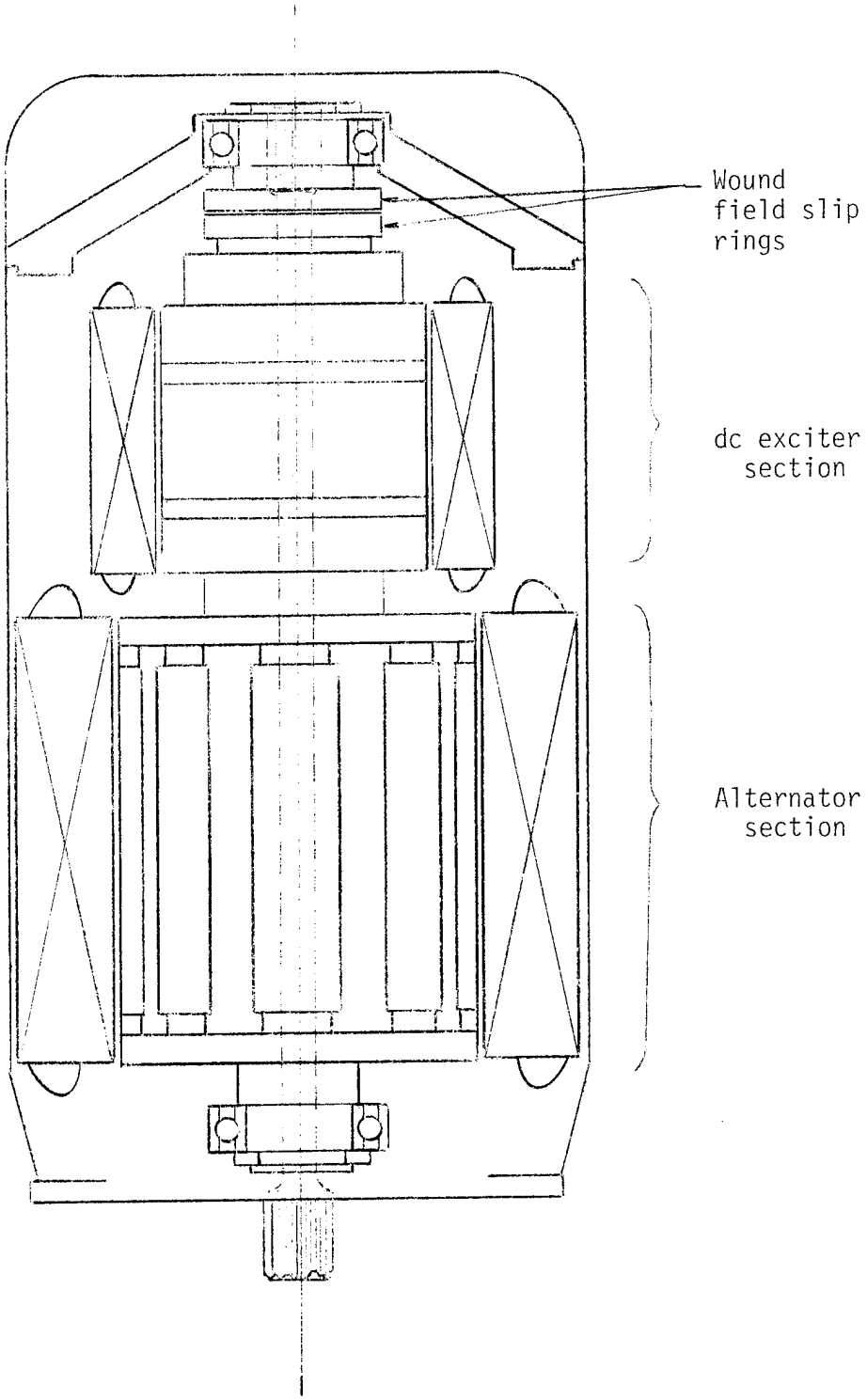

Figure 10. Existing Bendix 9kVA Alternator 1633-1A

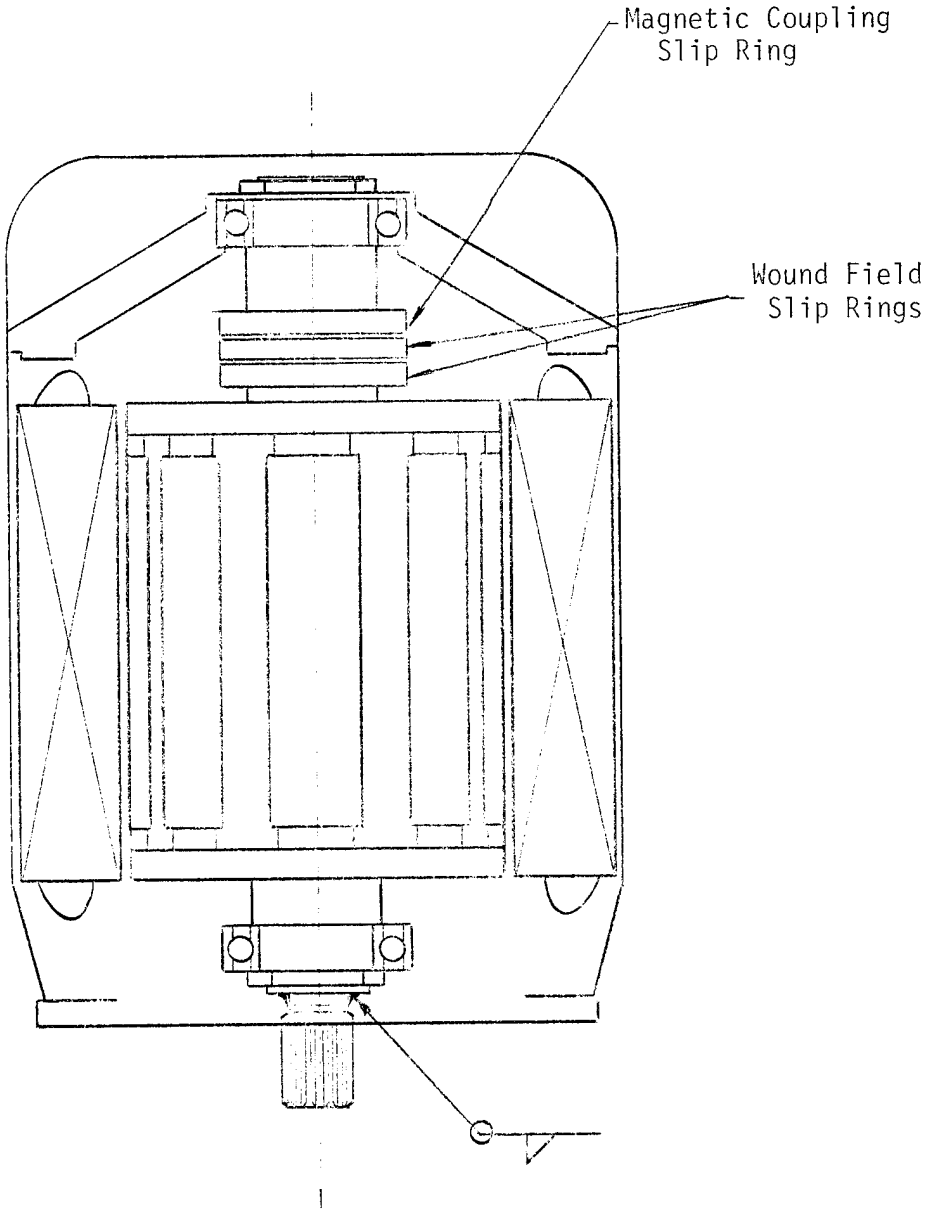

Figure 11.
Modified Bendix 9kVA Alternator: Slip ring added, dc exciter removed

power from the flywheel when the demand is greater than that available from the PV supply. For a given insolation and temperature of the PV cells, there is an optimum dc voltage where the maximum power is drawn from the PV supply. If the load demand increases above this maximum power output, it would cause the voltage output of the PV supply to drop excessively. This voltage drop will be opposed by power diverted from the flywheel if the output voltage of the generator is set at the optimum value. Similarly if the load demand decreases, the voltage of the PV supply tends to rise as the current falls. This rise in voltage and loss of current will also be prevented by having the output voltage set at the optimum value because as the PV output voltage rises, the generator becomes a motor and diverts power to the flywheel.

The FESS control system continuously monitors the dc bus voltage and sets it to a value which maximizes the power output of the PV supply. The set point voltage is produced through an integrated circuit pulse width modulator that regulates the field current of the generator. A schematic diagram for the control system is shown in Figure 12.

The circuit for the electronic commutation of the three-phase motor is also shown. A three-phase waveform generator develops the control signals for the six power transistors which drive the motor. The developed signal is a periodic three-phase square wave. The frequency of operation is a direct function of the rotor speed as the clock signal is generated from the rotor position sensor. The rotor position sensor is comprised of a number of optical sensors, a slotted position wheel, and some logic. As the slots pass through the sensors digital pulses are generated. The pulses are then combined to form the clock for the waveform generator. One of the sensor outputs also serves as the input to the synchro-switch as an aid in controling the magnetic coupling synchronization.

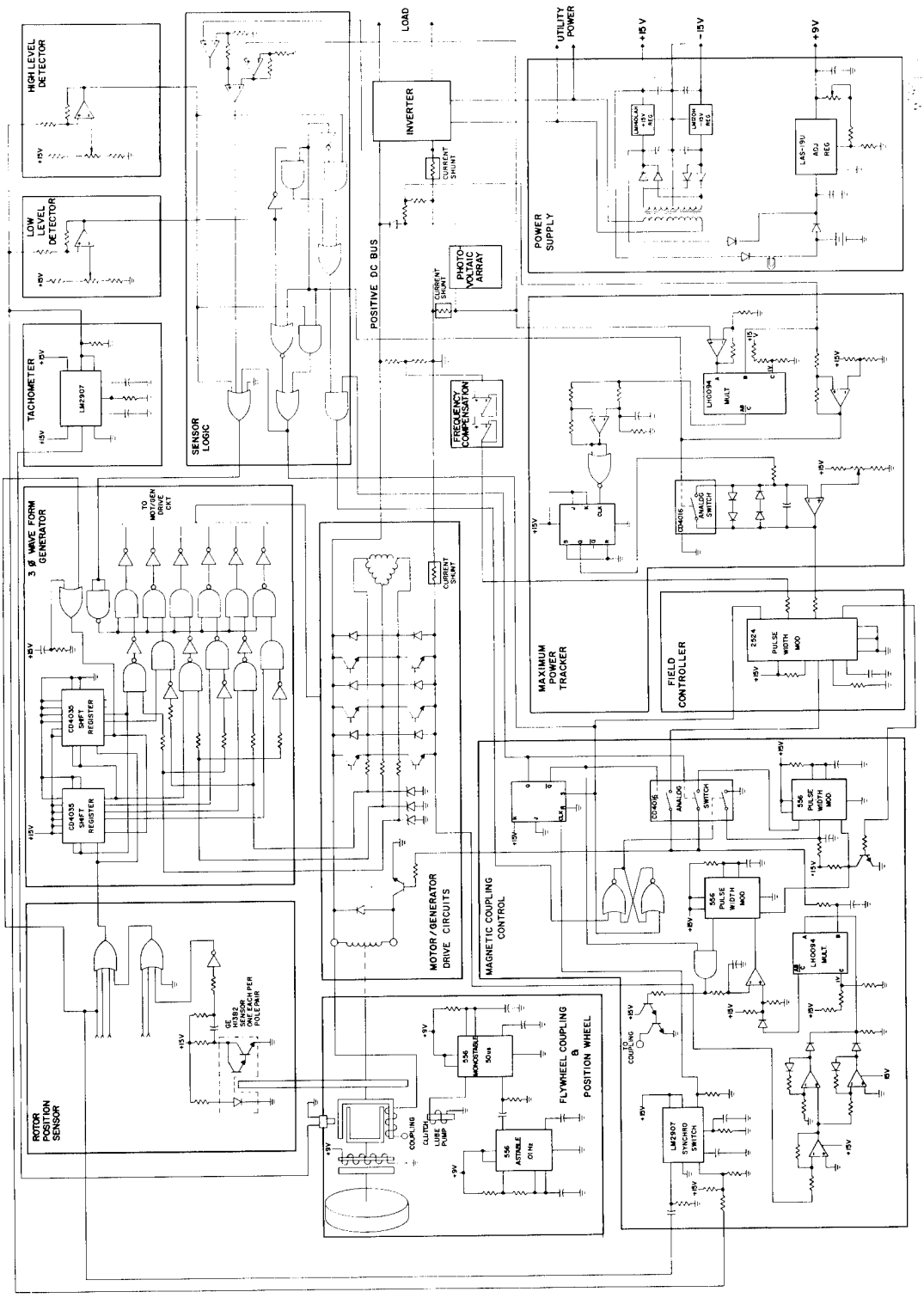

Figure 12. FESS Control Schematic

A unique feature is that the line voltage is monitored to prevent common devices from turning on simultaneously. This allows the conduction angle of the waveform to approach a maximum of 120°.

High and low level detectors are used as alarm signals that indicate abnormal velocities of the flywheel. Other than its normal operating range, the flywheel can be in one of two conditions. It can be discharged to the point at which little useful energy remains or it may be charged to the point at which no more energy can safely be added to the flywheel. The high or low level detector will indicate either of these states.

Field Controller

The Field Controller is an integrated circuit pulse width modulator that utilizes the bus voltage as feedback signal. The frequency of the field is fixed by discrete components at 4 kHz. The field is controlled by regulating the duty cycle of the 4 kHz to a value such that the feedback signal is equal to the modulator input. The result is that the bus is regulated to a value proportional to the input.

Maximum Power Tracker

The Maximum Power Tracker circuitry is used to set the operating voltage of the system to a point at which the maximum output power from the solar array is achieved. The circuit is operative only while the output of the array is above its minimum threshold; the circuit maintains the array power at its maximum power independent of its load. The characteristics of a typical solar cell at various concentrations are shown in Figures 13 and 14.

The power is controlled by adjusting the system bus voltage which in turn determines the operating voltage of the array. To determine the

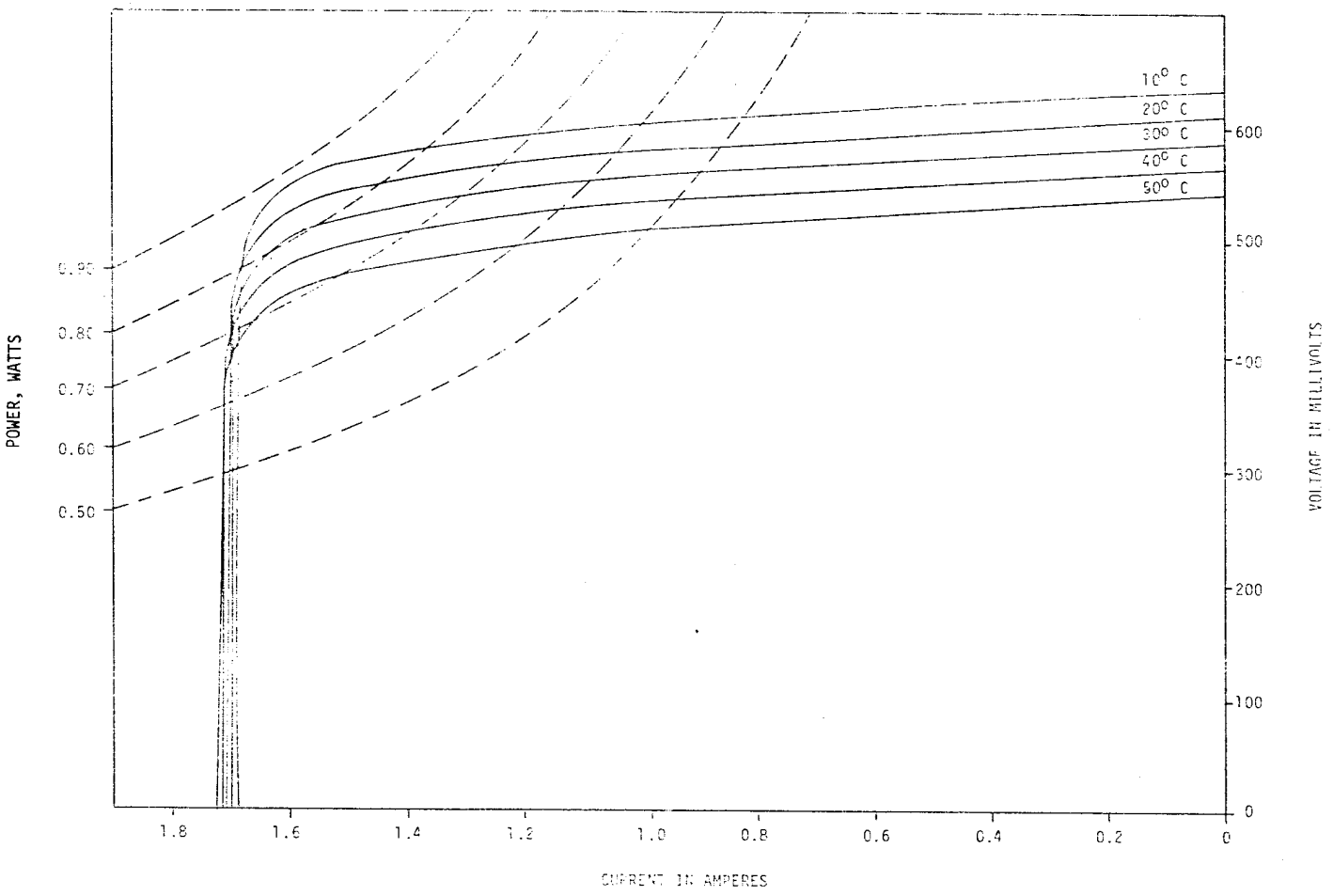

Figure 13. Voltage vs. Current @ .2 W/cm^2 Insolation (2 X)

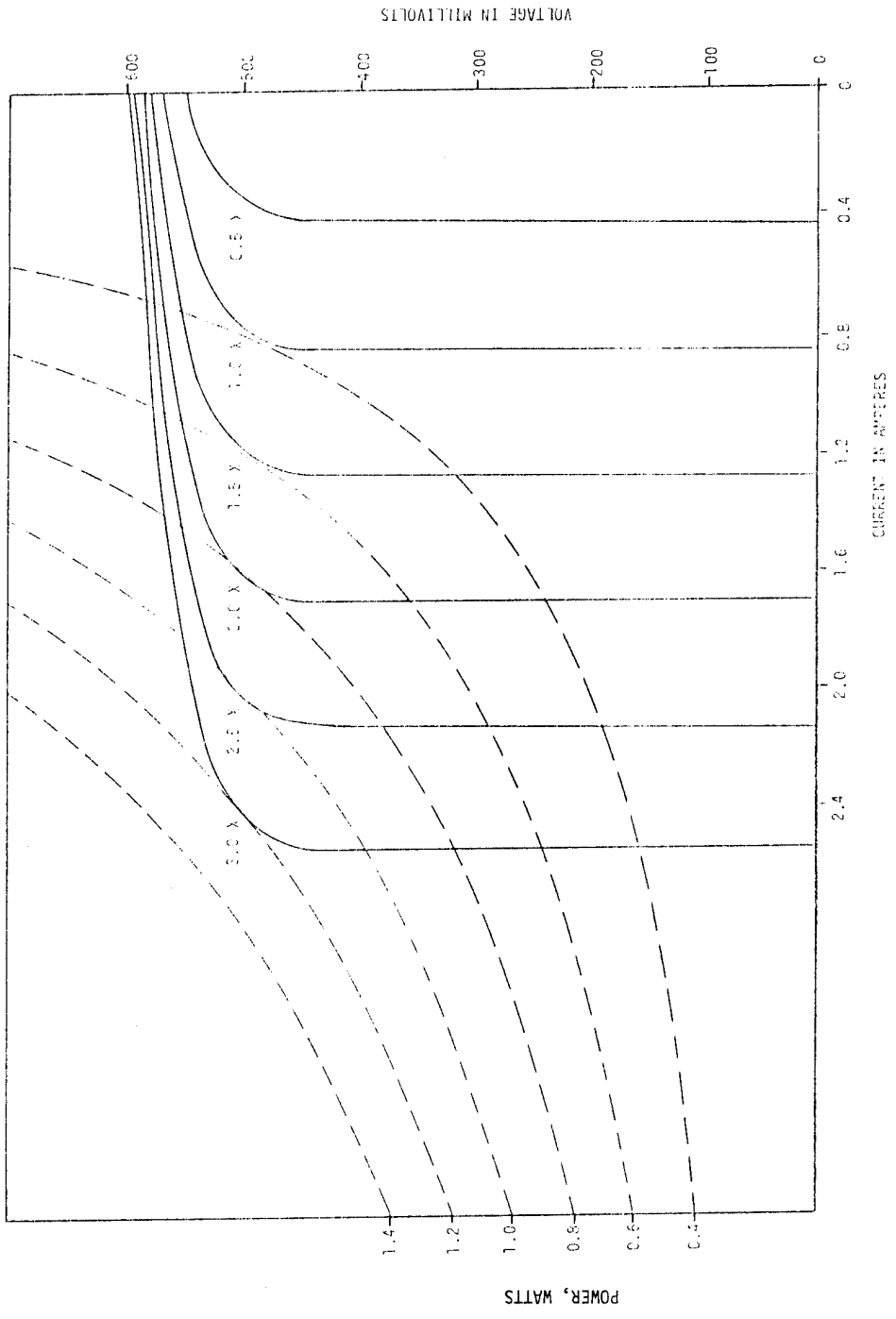

Figure 14. Voltage vs. Current @ 30°C Temperature

maximum power, the bus voltage is varied while the array power is monitored. The circuit adjusts the bus voltage to the point at which the array power is reduced. At this point, the polarity of the adjustment signal is inverted. The bus voltage is then adjusted in this new direction until the power is again reduced. By continually moving the set voltage the array power is maintained at its maximum power point.

Motor/Generator Drive Circuit

The power transistor circuit for driving the motor is shown in Figure 15. The drive electronics consists of NPN Darlington Transistors and diodes for the drive and generation modes. The transistors that are referenced to ground are driven directly through current amplifiers while the transistors that are referenced to the positive bus are driven from optical-isolators through current amplifiers. The optical-isolators are referenced to a voltage that is 5 Volts below the positive bus. This voltage is developed through an integrated circuit switching regulator.

Magnetic Coupling Control

When the magnetic coupling is in its normal operating mode, i.e., transmitting torque to or from the flywheel, the unit runs synchronously and its torque capacity is proportional to its excitation current. In this normal mode the magnetic coupling control circuit acts to regulate the excitation current to the level necessary to transmit the required torque. Regulation of the excitation current is achieved by use of a 4-kHz pulse width modulator with its pulse width determined by an integrated circuit that sets the required excitation current proportional to the product of the motor armature current and field current. Regulating the

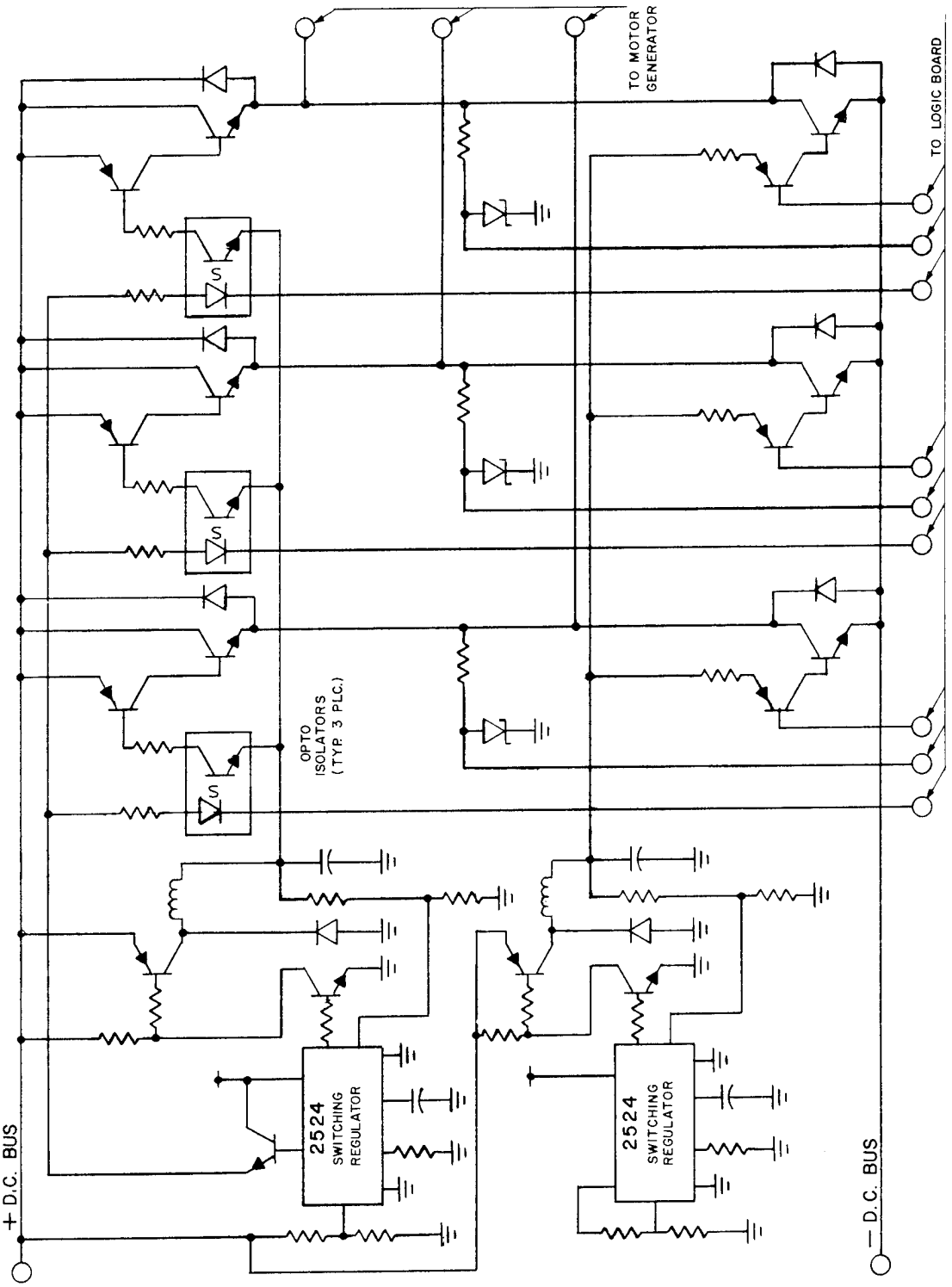

Figure 15. Motor/Generator Drive Circuit

excitation according to need limits the power loss in the coupling.

De-energizing the coupling allows the flywheel to coast free of the motor. In the de-energized mode the coasting flywheel has a minimum run-down loss. The flywheel would be in the "free wheeling" mode when no energy exchange is desired either because the flywheel is below its operating speed with no sunlight available or because it is in an overspeed condition with no power demand upon it. In either case the "free wheeling" continues until a change in conditions require that the coupling be re-energized.

In order to bring the coupling to its normal operating mode, following a de-energized period, synchronization of the coupling is required. Synchronizing the motor and flywheel is automatically controlled by raising or lowering the motor speed via control of the motor field current. The flywheel tachometer signal and the motor shaft position sensor signal are used as inputs to the synchro-switch IC which turns on the pulse width modulator to set the coupling excitation current to its appropriate level when synchronization occurs. During the period where the motor and flywheel speeds are being brought into synchronization the motor field current is controlled by the magnetic coupling control. After synchronization the motor field current is controlled by the maximum power tracker.

Sensor Logic

The sensor logic develops the command that directs the controller to either charge or discharge the flywheel and also to engage or disengage the coupling. The decisions of the sensor logic are made from information pertaining to the speed of the flywheel, the available solar power, and the required load.

Power Supply

The power supply driven from the utility line side of the inverter develops ±15 Volts and also +9 Volts to power the magnetic bearing and lube pump. The +15 Volts maintains a full charge on a 12-Volt gel-type storage battery. In case of a utility power failure, the auxiliary battery will drive the magnetic support and lube pump until the flywheel has run down or power has returned.

Inverter

The inverter is a purchased Gemini unit. The unit is of a synchronous type and, therefore, requires the presence of a utility line. An asynchronous inverter would be installed if a utility line is not present; however, due to the cost factor involved, it is felt that such an inverter should be included as part of the controller design.

COST ESTIMATE FOR THE TEN-kWh FESS

Layout drawings, specifications and cost estimates for serial production quantities of the 10-kWh, 5-kW FESS have been prepared based upon the developed concepts. Serial production costs are based upon estimates of costs for fabricating components to designs and methods of fabrication typical of mass-production techniques.

Prototype components are fabricated with a minimum of tooling, whereas, in high-production quantities expensive and elaborate tooling contributes little to part-production unit costs. In the quantity-production costs estimates the tooling cost has not been estimated and, in general, the material and production cost has been based upon the assumption of production quantities of 100,000 sets of parts where die costs are of

the order of a few cents per part. Then for each factor of ten reduction in quantity an increase of 17.6% in cost was assumed. This method of estimation is valid for three to four decades in quantity reduction but becomes unrealistic for small quantities where alternate methods of fabrication become dominant. Also it must be emphasized that what is defined as "production cost" does not mean "sales price" which will be higher by a factor of two to three depending upon marketing and amortization policies.

The cost of the mechanical assembly of the flywheel system was estimated on the basis of a design employing die-formed sheet-metal parts, rough-forged and machined steel parts, and permanent-mold and die castings, as applicable, for custom-made metal parts. Fiber-composite parts were estimated on a materials and labor basis for winding and curing using an up-date of fabrication costs from previous contracts. These costs were for rings of comparable weight and were extrapolated to larger numbers of components at 15% decrease for each factor of 10. Experience in winding biannulate rings confirmed the rate of build-up for fiberglass and Kevlar were approximately the same. Therefore, the cost per pound for the latter was taken as inversely proportional to density. Current material costs and quantity discounts were obtained from manufacturers of fiber and resin and were used with estimated waste allowances.

The cost of the aluminum hub was based upon materials and machining cost for a heat-treated, aluminum-alloy casting. For quantities of 100, a loose-piece-pattern, sand casting was assumed with the necessary draft and surface clean-up machining added. For larger quantities a permanent-mold

casting was estimated with substantial reduction in scrap and machining allowances. Neither technique of fabrication included the pattern (or permanent-mold) cost.

Metal parts, not including those in the rotor sub-assembly, i.e. hub and spoke weights, were estimated as categories by total finished weight, materials and processes. For example, one category included the main support shaft and its extension and the power output shaft. This category was estimated as high-carbon steel forgings, rough machined, heat-treated, ground to finish dimension and surface treated with a rust-resistant oxide coating. Costs of the various operations were based upon American Society for Metals examples for forging, finishing, etc., up-dated for current costs.

The most expensive category was that comprising the vacuum tank. Preliminary stress and deflection calculations indicated that sheet-steel stock thickness of 100 mils would be more than adequate for the tank heads if radial flutes were formed which terminated in a moment-transmitting attachment to a central mounting collar supporting the rotor-system weight. Alternative methods of forming such heads were drop-hammer or draw dies forming low-carbon steel sheet or the use of explosive-forming techniques for producing the flutes in a sheet-metal spinning supported in an open female die. The method chosen would depend upon quantity to be produced inasmuch as limited-life dies for small quantities could be made more cheaply than long-lived ones. The estimate for large-quantity production assumed a low die cost per unit produced which resulted in a formed part cost approximately twice the material cost. Forging, machining and welding

of the central mounting collar was separately estimated. In this same category was included the die formed sheet-steel parts supporting the lifting-magnet components, the main bearing and magnetic coupling supports.

The rotating electrical components, namely the magnetic coupling and the motor generator, were estimated separately. The magnetic coupling cost was based upon wholesale price of a three-phase induction motor of a comparable torque rating. Lamination and winding costs were considered comparable and the difference between wholesale price and original-equipment-manufacturers (OEM) cost (about a factor of two) covered the special features of slip rings, vacuum barrier, etc. This cost was considered representative for quantities of 100,000 and was increased for reduced quantities in the manner previously described.

The cost of the motor-generator was based upon the wholesale price of an electronically-excited, commercial alternator of a kilowatt rating, adjusted for difference in speed of minimum flywheel speed of 5,000 rpm and standard alternator speed of 3,600 rpm. These estimates were also escalated with decreasing quantity in the above-described manner.

The cost per assembly is shown in Table 2.

Table 3 shows the estimated costs for controller in various quantities. The cost of parts is sensitive to the cost of high power switching devices. These devices are experiencing significant decreases in price and the parts cost picture may actually look even better in the future. Using present costs, in 100,000 production quantities, the $412 controller-peak power tracker costs represent a cost of $82 per switched kilowatt. This cost also covers the many other functions of the controller (speed sensing, magnetic lift control, magnetic clutch control, peak power tracker, etc.).

Table 2. Cost Per Assembly - 10-kWh 5-kW FESS Mechanical Assembly

NO. OF ASSEMBLIES	FABRICATED COMPOSITES COST $	ASSEMBLED ROTOR COST $	COMPONENT CATEGORY(1) (a) COST $	(b) COST $	(c) COST $	(d) COST $	(e) COST $	MISC. HDWE. COST(2) $	MAGNETIC COUPLING COST $	ALTERNATOR COST $	TOTAL PARTS COST $	ASSEMBLY LABOR COST(3) $	TOTAL(5) COST PER ASSEMBLY(4) $
10^2	3429	4575	28.50	64.30	346.00	113.70	0.98	159.25	266.20	895	6449	646	7085
10^3	3011	3828	24.20	54.70	294.10	96.60	0.82	150.95	226.30	760	5437	408	5845
10^4	2643	3343	20.60	46.50	250.00	82.10	0.80	133.50	192.35	650	4719	236	4955
10^5	2455	3055	17.50	39.50	212.50	69.80	0.80	123.20	163.50	550	4232	213	4445

(1) a. Heat treated ground steel components; b. carbon steel ground components; c. formed sheet steel components; d. machined fabrications; e. die castings.

(2) At 10 percent of component category cost + ball bearing sets.

(3) At 10 percent, 7.5 percent, 5 percent, 5 percent respectively of total parts cost.

(4) Does not include development or tooling costs.

(5) 1979 Dollars

Table 3. 10-kWh (5-kW) Controller Cost Estimate

(Cost in 1979 Dollars)

QUANTITY	PARTS	ASSEMBLY	TOTAL
10^2	472.84	63.02	535.86
10^3	418.29	60.13	478.32
10^4	384.86	56.15	441.01
10^5	360.44	51.65	412.01

Table 4 shows the estimated 10 kWh total system cost for various quantities of production. In quantities of 100,000 units per year, the total production cost is estimated to be $5057 or $505 dollars (1979) per usable kilowatt-hour stored.

Table 4. Cost Estimate for 10-kWh FESS

QUANTITY	MECHANICAL PARTS	CONTROLLER PEAK POWER TRACKER	INVERTER	TOTAL
10^2	7085	536	795	8416
10^3	5845	478	276*	6599
10^4	4955	441	235	5631
10^5	4445	412	200	5057

*Represents the change from a commercially purchased unit to an in-house design.

SUBSYSTEM SELECTION CRITERIA

ROTOR MATERIALS

In order to minimize costs, the material must have high energy storage per dollar of cost. Energy storage per dollar of material is directly proportional to the strenth-to-weight ratio divided by the cost per pound.

Flywheel rotor material must have a high strength-to-weight ratio in order to keep down the size of the rotor. This keeps down the rotor weight which minimizes bearing loads. Another advantage is that the enclosure size is kept to a minimum.

In addition to high strength, high fatigue strength is also necessary because the unit must have a long life with a large number of charge/discharge cycles. If the material is a fiber-composite then the static fatigue strength must also be high because the unit is required to operate for twenty years.

Total manufacturing costs are to be minimized. Because of this the cost of fabricating the material must be low.

Two types of materials were considered: isotropic (metal) and orthotropic (fiber-composites).

Because of the high strength-to-weight ratio requirement only high strength steels were considered for the isotropic material. Three fibers were considered for the orthotropic material: E-glass, S-glass, and Kevlar. For all three, epoxy is the matrix material.

Table 5 lists the types and properties of steels that were considered.[4] The fiber properties are listed in Table 6.[5]

A detailed cost analysis was done to determine the relative cost of a steel rotor vs. a composite rotor.

The steel rotor considered is shown in Figure 16. It is a truncated cone with no hole in the center. The material is A471 Class 9 steel that is heat treated to the requirements of A723.

The composite rotor rim is shown in Figure 17. It is a ring composed of S-2 fiberglass in an epoxy matrix.

The manufacturing costs of both rotors are shown in Table 7. Note that for the composite ring the costs decrease sharply as the number of units produced increases. For the steel disk, however, cost remains almost constant for any number of units produced. This result shows clearly the economic advantage of fiber-composites for flywheel rotors.

Of three composites considered, E-glass is the least expensive. It has the lowest strength but the ratio of its strength to cost make it an attractive candidate. S-glass is approximately 1.5 times stronger than E-glass and Kevlar is approximately twice as strong as E-glass.

The cost of S-glass is approximately five times that of E-glass. Kevlar costs approximately 18 times as much.

Figure 18 shows the cost of a rotor made from each composite as a function of fabrication costs. Note that E-glass rotors have the lowest cost if fabrication costs are below approximately $2.50 per pound. Above $2.50 per pound, S-glass rotors have the lowest cost.

TABLE 5. Steel Properties

STEEL	DENSITY LB/IN^3	TENSILE K LB/IN^2	YIELD K LB/IN^2	COST $/LB
HP-9-4-20	.283	190	180	2.21 (1)
HP-9-4-30	.283	230	210	2.21 (1)
UNIMACH AF1410	.283	235	220	3.40 (1)
18NI-250 MARAG	.289	270	---	2.25 (1)
18NI-300 MARAG	.289	260	---	2.30 (1)
18NI-400 MARAG	.289	275	---	2.35 (1)
4340	.283	260	---	1.25 (1)
C1141	.282	237	---	0.50 (1)
A471	.283	170	160	4.66 (2)
A723	.283	190	180	4.66 (2)

(1) Billet Price

(2) Forged, Rough Machined and Heat Treated Price

TABLE 6. Fiber Composite Properties (Nominal)

Fiber:	E-Glass (Owens-Corning)	S2-Glass (Owens-Corning)	Kevlar 49, 1420 Denier
Vol% Fiber:	Nominally 65%	Nominally 60%	Nominally 60%
Density:	.0117 lb/in^3	.0116 lb/in^3	.0077 lb/in^3
Mechanical Properties			
Elastic Constants:			
Longitudinal Young's Modulus	7.6 x 10^6 lb/in^2	8.2 x 10^6 lb/in^2	11.9 x 10^6 lb/in^2
Transverse Young's Modulus	2.0 x 10^6 "	2.3 x 10^6 "	7.4 x 10^6 "
Shear Modulus, G_{12}	0.9 x 10^6 "	1.1 x 10^6 "	2.6 x 10^6 "
Major Poisson's Ratio	0.207	0.282	0.310
Minor Poisson's Ratio	0.056	0.079	0.193
Ultimates:	Tension	Tension	Tension
Longitudinal Strength	160 K lb/in^2	234 K lb/in^2	268 K lb/in^2
Longitudinal Ultimate Strain	2.2%	2.9%	2.2%
Transverse Strength	1.1 K lb/in^2	5.9 K lb/in^2	1.1 K lb/in^2
Transverse Ultimate Strain	0.054%	0.292%	0.16%
	Compression	Compression	Compression
Longitudinal Strength	77 K lb/in^2	67 K lb/in^2	34 K lb/in^2
Longitudinal Ultimate Strain	1.1%	0.92%	0.48%
Transverse Strength	11.3 K lb/in^2	16.2 K lb/in^2	7.7 K lb/in^2
Transverse Ultimate Strain	0.68%	2.93%	1.4%
Shear Stress at 0.2% Offset	3.2 K lb/in^2	4.4 K lb/in^2	3.5 K lb/in^2
Shear Strain at 0.2% Offset	0.55%	0.62%	1.55%

Matrix: 100 parts Dow Chemical DER 332 (bisphenol-A epoxy resin), 45 parts Jefferson Chemical Jeffamine T403 (polyether triamine)

Cure: 16 hours @ 60°C (E-Glass & S2-Glass)
Cure: One day at room temperature and 16 hours at 85°C (Kevlar 49)

Reference: L. L. Clements and R. L. Moore, Lawrence Livermore Laboratory, Report UCRL-79262, 1977 (SI units converted to English units)

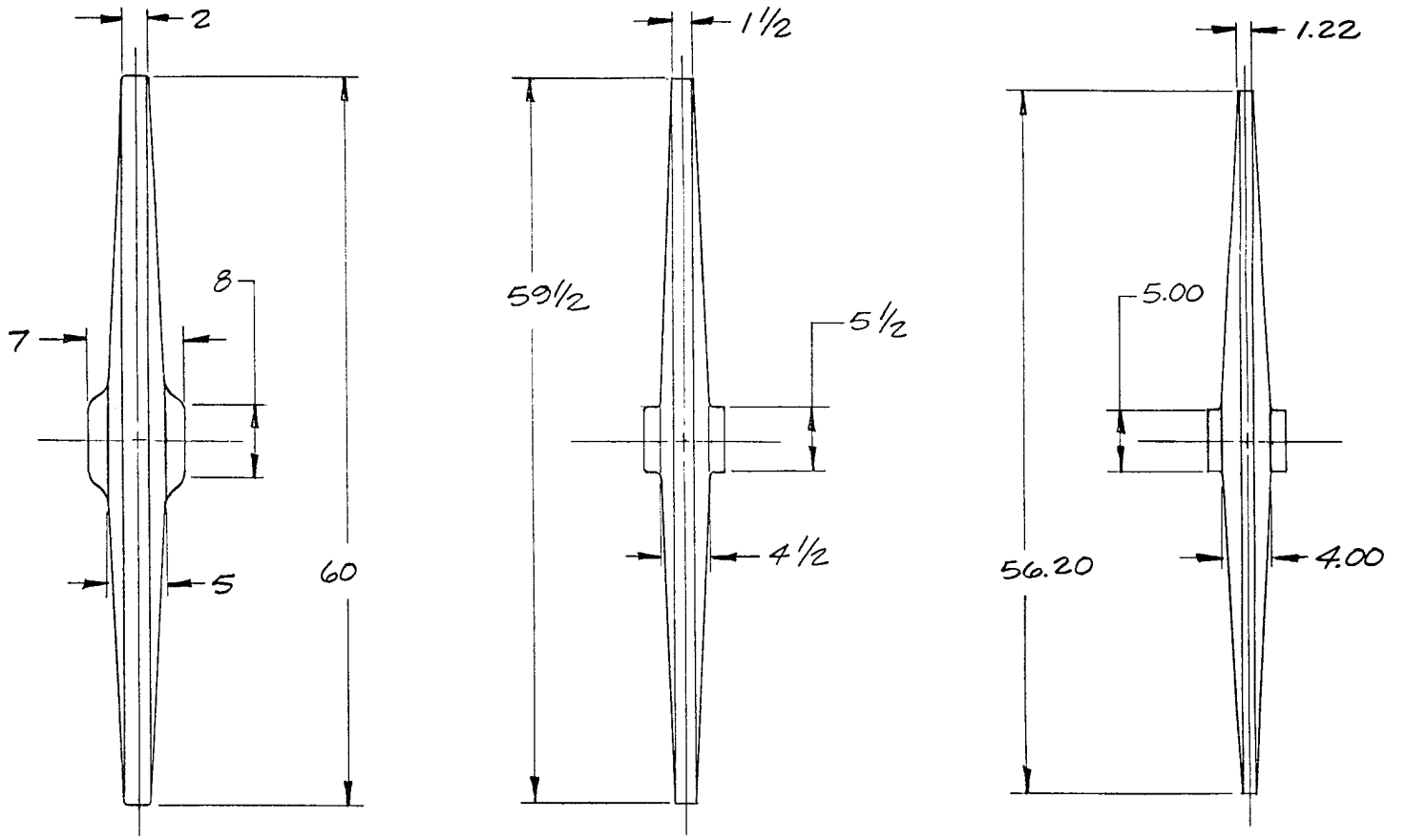

A471 CLASS 9 STEEL

DESIGN 2 - ENERGY STORAGE COMPONENT
(DIMENSIONS IN INCHES)

Figure 10. Steel Rotor - Truncated Cone

DR.BY: K.S.LANGE
DATE: 12.6.78

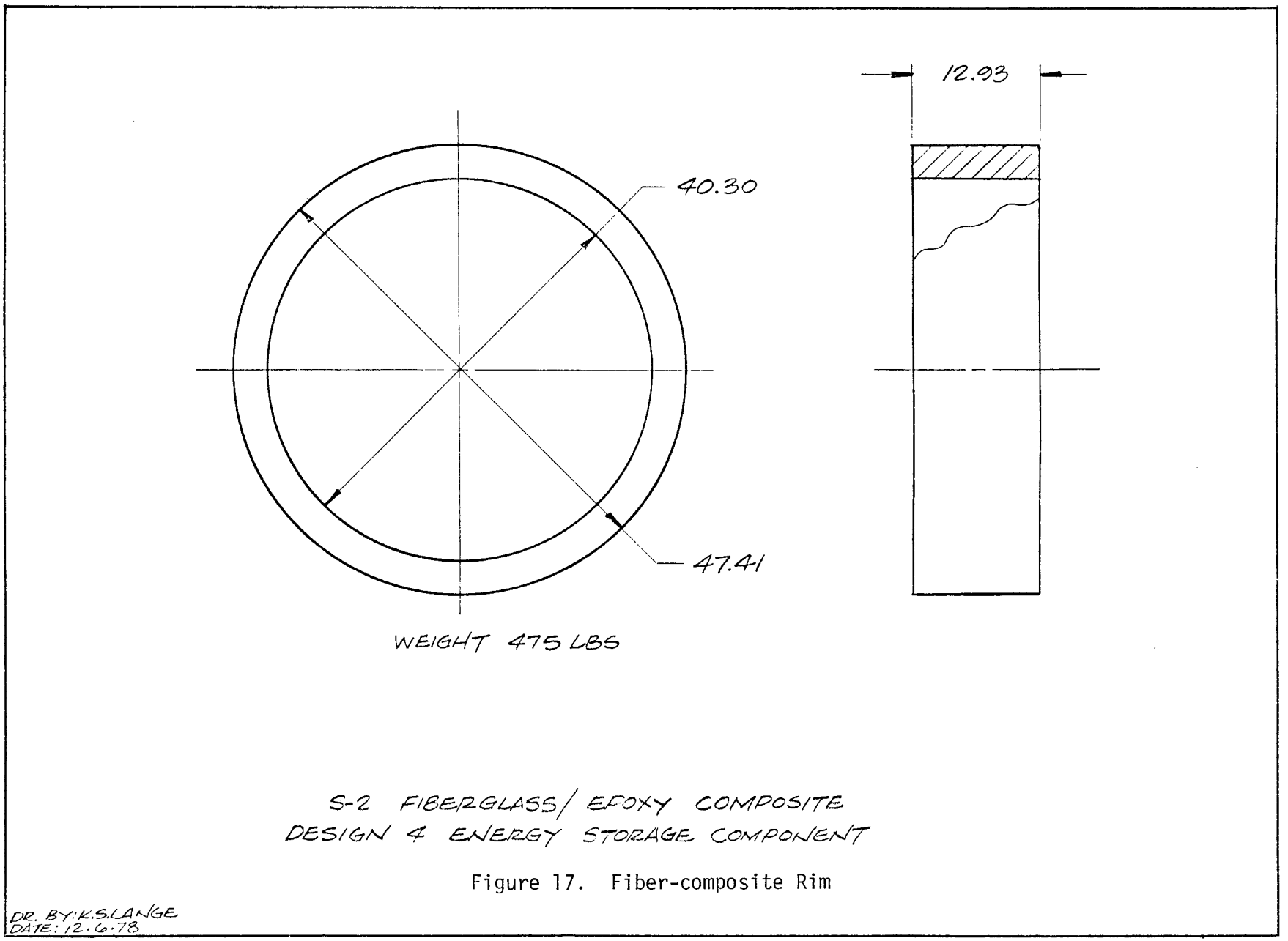

Figure 17. Fiber-composite Rim

TABLE 7. Cost Comparison - Composite Ring vs. Forged Disc
(1979 Dollars)

No. of Units	Composite Ring			Forged Disc		
	Cost/Ring	Unit Cost		Cost/Disc	Unit Cost	
	$	$/lb	$/kWh	$	$/lb	$/kWh
10^0	13,775	29.00	1,020	16,841	11.20	1,247
10^1	4,171	8.78	309	15,662	10.41	1,160
10^2	2,722	5.73	202	15,529	10.33	1,150
10^3	2,465	5.19	183	15,518	10.32	1,149
10^4	2,367	4.98	175	15,517	10.32	1,149

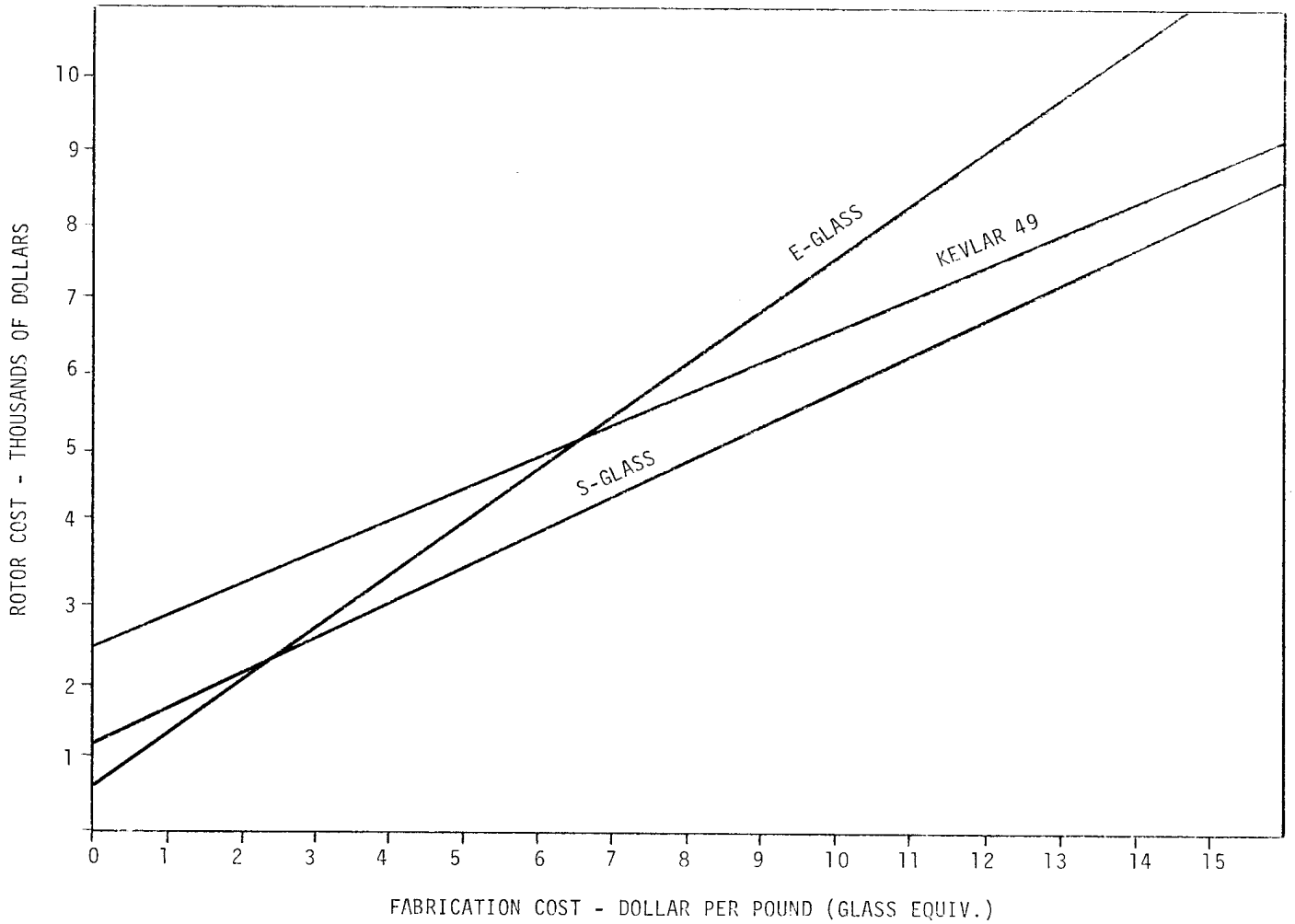

Figure 18. Rotor Costs - 13.5-kWh Composite Flywheels

Figure 19 shows the fabrication cost per pound as a function of quantity for fiberglass epoxy rings. Note that when the quantity exceeds 100 units, the fabrication costs are below $2.50 per pound. This shows that for high volume production, E-glass is the most economical material.

ROTOR SHAPES

Rotor design requirements included:

- The maximum operating speed is below 10,000 rpm to simplify motor selection
- Low stress levels to ensure reliability
- Low cost
- Reasonably compact size in order to minimize enclosure cost
- Short axial length in order to avoid instability problems

A number of rotor shapes were examined. Candidate shapes included:

- Constant stress disk
- Modified constant stress
- Multi-disk
- Truncated conical disk
- Flat disks, pierced or unpierced
- Thin ring
- Rim with web and hub
- Multi-ring (concentric rings)
- Radial rod ("super flywheel")

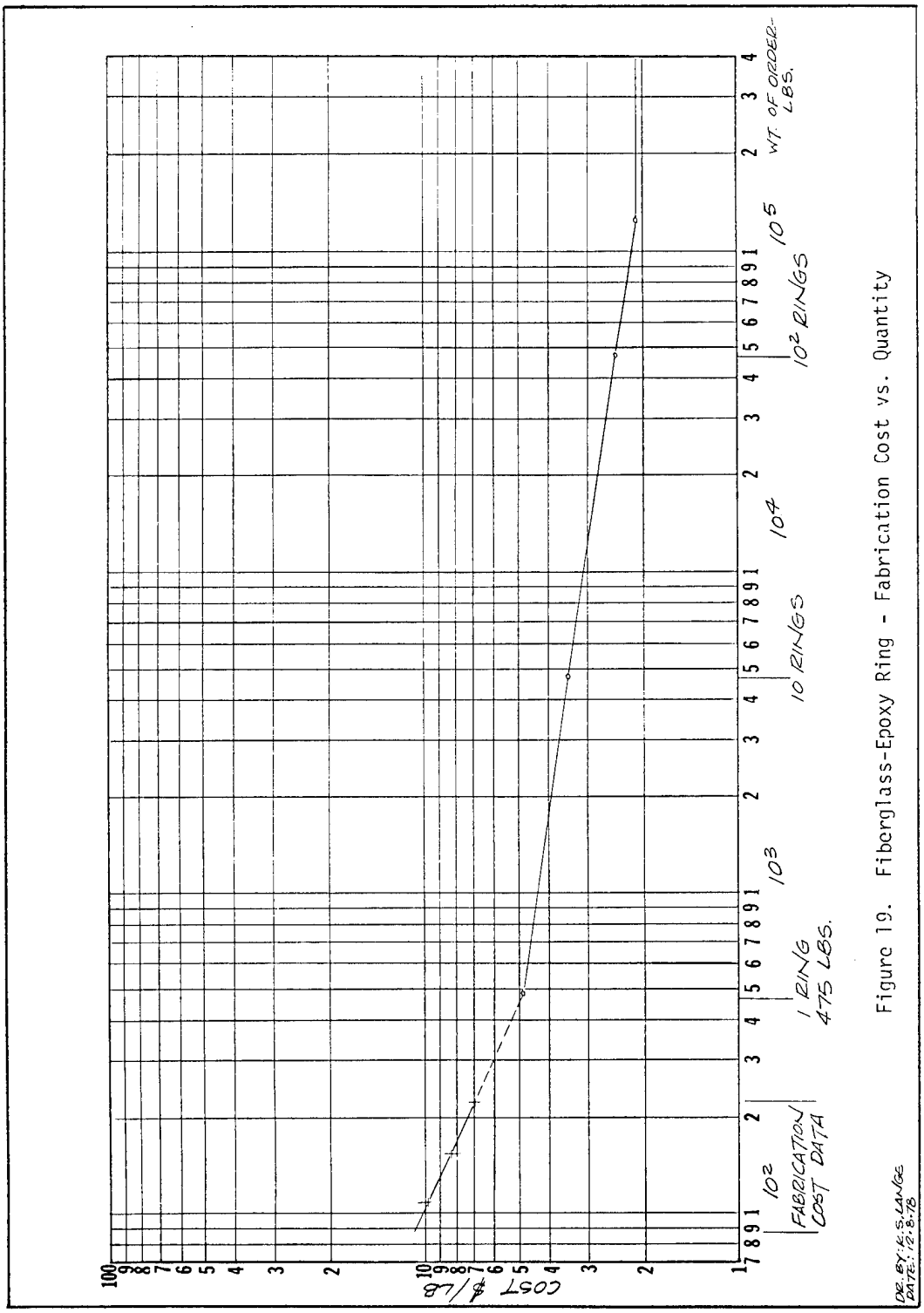

Figure 19. Fiberglass-Epoxy Ring - Fabrication Cost vs. Quantity

The optimum rotor shape for an isotropic material is different than that for an orthotropic material. The isotropic material is capable of supporting high stresses in all directions. An optimum design would take advantage of this capacity by imposing equally high radial and circumferential stresses as in the constant stress disk. The truncated conical disk also supports high radial and circumferential stresses although not exactly of equal value. Because the stresses in the truncated conical disk are not strictly uniform, the maximum energy which can be stored is about 80 percent of that for the modified constant stress disk. However, as the fabrication costs of the various shapes are considered; the one giving the greatest energy storage per dollar for isotropic materials is then compared to the best orthotropic design.

Orthotropic materials can carry high stress in only one direction and are best used in shapes which take advantage of that characteristic. The thin ring designs impose circumferential stresses which are nearly uniform whereas the radial-rod designs impose radial stresses which are high at the center and drop to zero at the outer edge. The uniformly high stress in the thin ring carries the highest energy per pound of material, but does not provide a good utilization of space. Increasing the radial thickness of the ring improves the space utilization but increases the radial tensile stress. Since the composite strength is low in tension in the radial direction, the thickness cannot be increased by a large amount.

Economic considerations show clearly the advantage of using E-glass for the rotor material. But the high modulus of elasticity and low density of the more expensive Kevlar 49 makes it the ideal material for use as a thin overwrap.

This combination of properties assures that the Kevlar outer portion will act as a reinforcing band about the E-glass to maintain radial compressive stresses. This arrangement permits the combined rim to have the large radial thickness required to achieve a good space utilization. The radially thick rim is also easier to support than a thin one because the ratio of the rim inside diameter to the hub diameter is smaller.

A biannulate rim, consisting of an inner ring of E-glass/epoxy with an overwrapped outer ring of Kevlar 49 permits a considerable increase in radial thickness for the complete rim without giving excessive radial tensile stress. This large radial thickness also gives good space utilization. The ratio of Kevlar to fiberglass in the biannulate rim was determined by design studies. Only a small amount of Kevlar is required to give an optimum design.

Figures 20 and 21 show the tangential and radial stress of the 10-kWh rotor (49.88-in O.D. and 40.88-in I.D.) at the maximum rotational speed of 9,800 rpm. Maximum tensile stress is 112,000 psi in the E-glass and 141,000 psi in the Kevlar. Maximum radial stress is 1,000 psi tension in the E-glass and 820 psi compression in the Kevlar. Stresses were calculated using equations given by Timoshenko.[8]

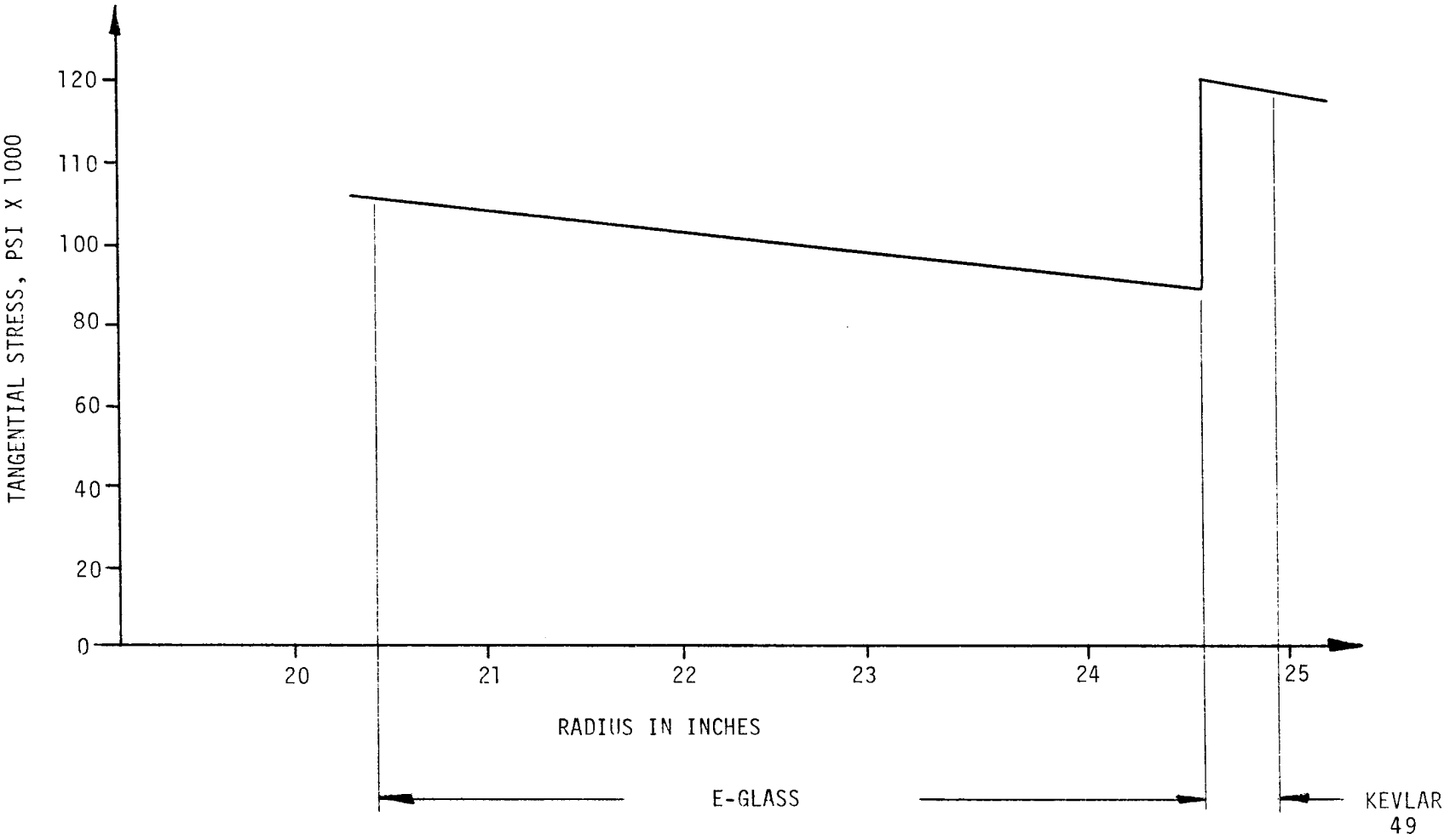

Figure 20. Rotor Rim Tangential Stress vs. Radius - 10,000 rpm Rotational Speed

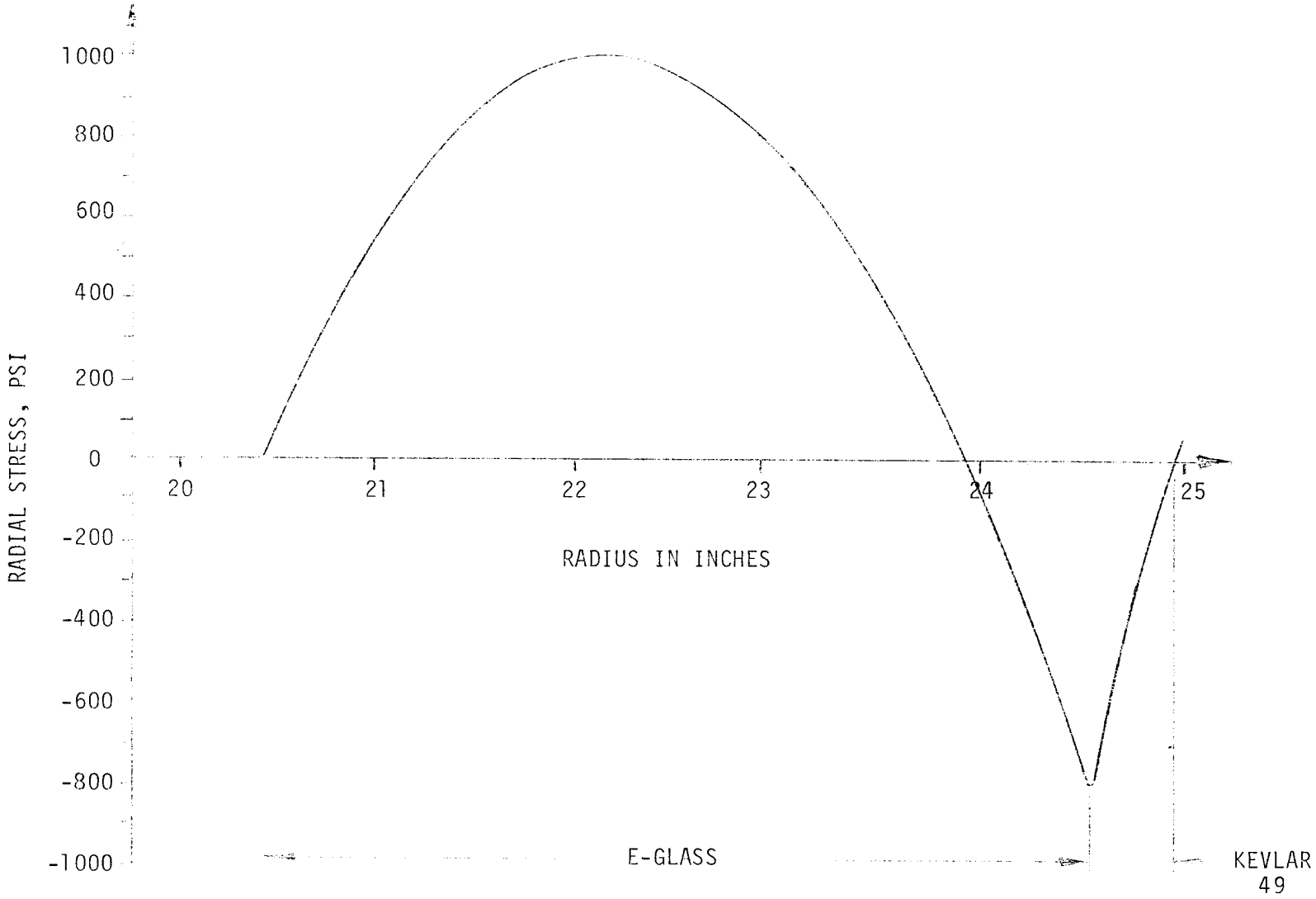

Figure 21. Rotor Rim Radial Stress vs. Radius - 10,000 rpm Rotational Speed

Rim support is provided by polar catenary spokes. These spokes are tension-balanced to reduce undesirable radial loading on the rim. The spoke material, Kevlar 29, was selected to give acceptable stress levels and to produce a rigid support to maintain alignment of the rim and hub. The maximum tensile stress in the spokes is 90,800 psi.

The hub provides support to the spokes. The hub material is aluminum with a Kevlar overwrap. An interference fit puts the aluminum rim into compression when the hub is not rotating. This pre-stressing limits the tangential tensile stress in the aluminum to an acceptable value at the maximum rotation speed.

Figures 22 and 23 show the tangential and radial stress in the rim at 0 and 10,000 rpm. Maximum tangential stress in the aluminum is 10,000 psi compression at 0 rpm and 10,000 psi tension at 10,000 rpm. Maximum radial stress is 800 psi compression at 0 rpm and 1,230 psi compression at 10,000 rpm.

HOUSING AND CONTAINMENT

This component serves a number of important functions:

- An evacuated enclosure to reduce windage losses.
- An encasement to prevent corrosion and mechanical damage to the flywheel.
- A structural member to transmit load.
- A means of containment in the event of failure of the wheel or bearings.

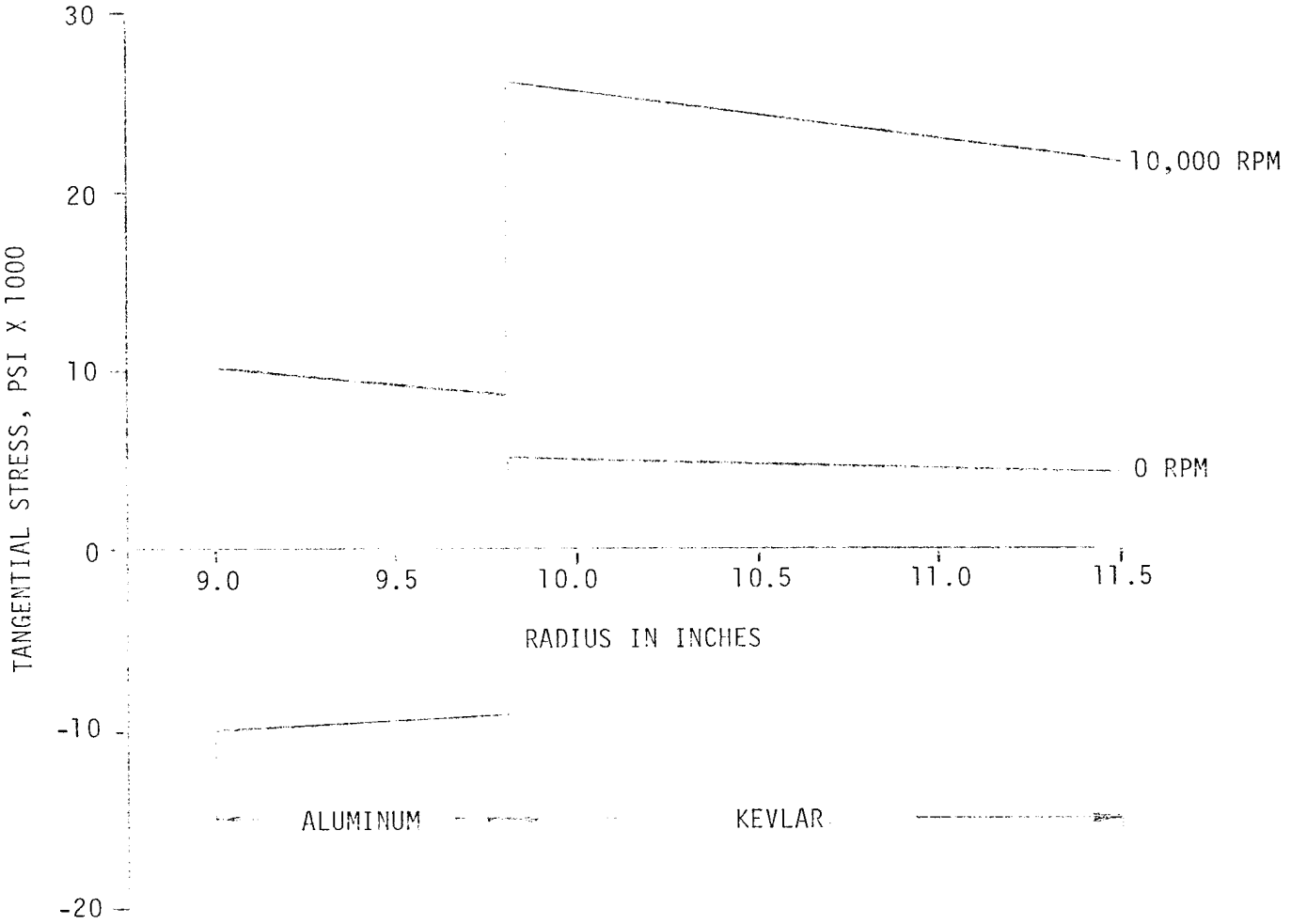

Figure 22. Hub Tangential Stress vs. Radius

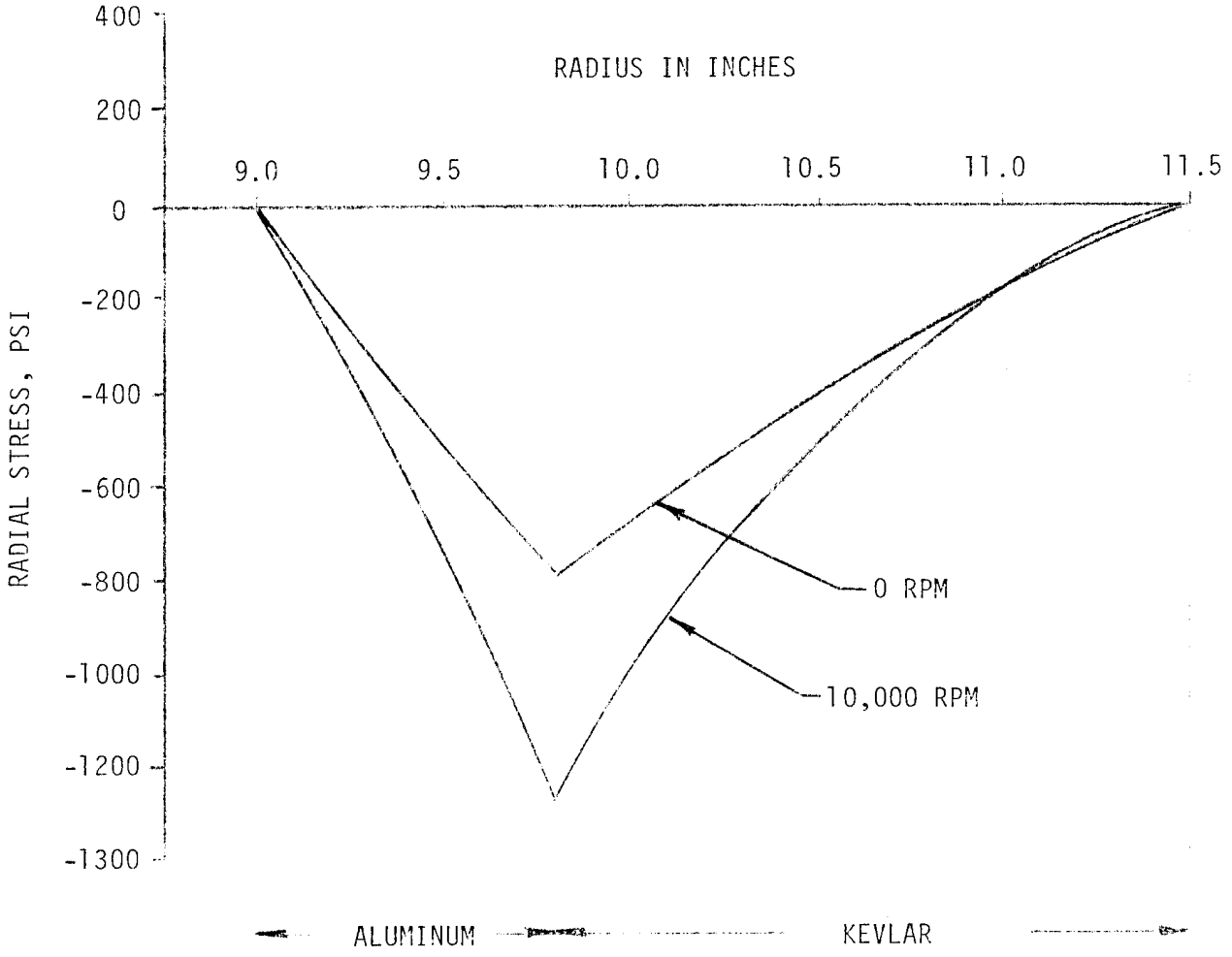

Figure 23. Hub Radial Stress vs. Radius

The most difficult requirement is to contain a failed rotor. To satisfy this, three concepts were considered:

- A thick steel container
- A thin steel container with a fiber overwrap
- A thin steel container in a concrete-lined pit

An economic analysis was done to compare the relative costs of each concept. The results in Table 8 show that the most economical approach is a thin steel container in a concrete-lined pit.

MOTOR/GENERATOR SELECTION

The motor/generator (M/G) unit which is used to couple power into and out of the flywheel must fulfill a unique set of requirements. As the name suggests, the unit has to be capable of efficient operation in both motoring and generating modes. The M/G unit must be able to run over the wide range of flywheel speeds. Full power (5 kW) is required from 5,000 to 10,000 rpm and operation to 0 rpm is required in the motoring mode. The speed of the unit should be easily controlled to avoid costly exotic controller schemes. As the design life of the flywheel energy storage system is 20 years, the motor/generator must be designed for long life with minimum service requirements. Due to high system efficiency requirements, the motor/generator unit must have very low losses. Lastly, the unit must be reasonably priced.

TABLE 8. Containment Cost Comparisons

Description	Cost[1]
Thick steel	$5292
Thin steel and fiber overwrap	$2565
Thin steel in concrete-lined pit	$1705

[1] Costs include installation

Given the above requirements, the following motor types were chosen for evaluation.

1. Direct current brush and commutator type
2. Permanent magnet synchronous
3. Wound rotor synchronous
4. Squirrel cage induction
5. Inductor
6. Multiple windings on rotor

The dc (brush and commutator) motor is easily controlled, and automatically adapts to the dc solar sourced power. Efficiency is also good but projected lifetime and maintainance requirements are unattractive. The permanent magnet synchronous machine, while providing high reliability and lifetime, is expensive and requires extensive outside circuitry for voltage control. The wound rotor synchronous machine is an electronically-commutated device with excellent voltage control capabilities. Its cost is acceptable and lifetime, reliability and efficiency are good. The squirrel cage induction motor is known to require complex and expensive circuitry for operation as a motor and generator. The voltage control characteristics are also poor. The inductor-type machine typically exhibits an efficiency which is too low for this application. The multiple winding devices require elaborate power switching networks and tend to be very expensive.

Table 9 shows a summary of the candidates' qualities. Appropriate weighting factors are shown at the bottom of the columns and summed results are shown in the right column.

TABLE 9. Motor/Generator Comparisons

MOTOR TYPE	DUAL FUNCTION AS MOTOR AND GENERATOR	COMPETITIVE PRICE ($/KW)	ADAPTABLE TO FLYWHEEL USE		LONG LIFE	RELIABILITY	HIGH EFFICIENCY	OVERALL GRADE
			HIGH TIP SPD (FT/MIN)	CONTROLLABLE VOLTAGE				
DC	EXCELLENT 4	FAIR 2 ($200 TO $300)	FAIR 2 (20,000)	EXCELLENT 4	POOR 1	FAIR 2	GOOD 3	22.5
PERMANENT MAGNET SYNCHRONOUS	EXCELLENT 4	POOR 1 ($250 TO $300)	GOOD 3	POOR 1	GOOD 3	EXCELLENT 4	GOOD WORKING POOR COASTING 2	20.0
WOUND ROTOR SYNCHRONOUS	EXCELLENT 4	FAIR 2	GOOD 3 (15,000 SALIENT POLE)	EXCELLENT 4	FAIR 2	GOOD 3	EXCELLENT 4	26.0
SQUIRREL CAGE INDUCTION	POOR 1 DIFFICULT TO SUPPLY FIELD EXCITATION	EXCELLENT 4 ($55 TO $65)	EXCELLENT 4 (30,000)	POOR 1	EXCELLENT 4	EXCELLENT 4	GOOD 3	20.5
INDUCTOR	GOOD 3	FAIR 2	GOOD 3 (<30,000)	GOOD 3	GOOD 3	GOOD 3	POOR 1	19.5
MULTIPLE WINDINGS ON ROTOR	GOOD 3	POOR 1	POOR 1	EXCELLENT 4	GOOD 3	GOOD 3	FAIR 2	20.0
	X 1.5	X 1.0	X 0.5	X 1.5	X 1.0	X 1.0	X 1.5	(WEIGHTING)

As seen in the table, the best motor/generator candidate for the flywheel energy storage system is the wound rotor synchronous motor.

For use on the solar sourced dc bus, this type of motor requires a position sensor on the armature and an electronic commutation system. Voltage and speed control are easily accomplished by adjusting field excitation (supplied to the armature by slip rings). The electronically-commutated separately-excited motor/generator operates at unity power factor which makes more efficient use of the power switching devices than does the induction device which operates at various power factors (depending upon load and speed).

As the prototype FESS is intended to be designed around off-the-shelf items, an extensive search was made of motor manufacturers to find an existing unit which would meet the requirements. An interesting problem surfaced. High speed motors of this type generally fell into two categories. One is the high speed motor with very elaborate bearing and shaft assemblies designed to rigidly hold grinding wheels. The motor itself is a minor part of these grinding spindle assemblies and, as such, the unit costs are quite high. The other available type of unit is the aircraft alternator. These units are designed with an emphasis on extreme light weight and are also quite expensive. For large quantity production, a low-cost unit without the emphasis on weight or extreme precision will have to be built. An aircraft unit with the following specifications was selected for the prototype unit:

BENDIX AC GENERATOR NO. 1633-1A

9 kVA Peak Output
208 Volt Nominal
Three-phase
1000 Hz @ 10,000 rpm

This unit will require some modifications for use in the FESS which include removal of the dc exciter section and the addition of a third slip ring for the magnetic coupling excitation.

CONTROL SYSTEM

Circuit Logic

Two options were considered for the circuit design: linear circuitry and microprocessor circuitry. Because all the control functions are linear, linear circuitry is used. Also, the unit production cost of linear circuitry is much less than microprocessor in small production quantities. Even for quantities as large as 100,000, cost advantage of either option is not clear.

Power Devices

Three types of power devices were considered:

1. Transistors
2. Thyristors or SCR's
3. Power field effect transistors

Transistors have high frequency response which lowers switching losses. They can be easily commutated which results in simpler circuitry.

Thyristors are inexpensive and have high power ratings. But their frequency response is low and they require rather complex circuitry for commutation.

Power field effect transistors combine the advantages of the other two elements (with the possible exception of being inexpensive). They have a high power rating, high frequency response and they are easily commutated. They are also quite efficient because they require zero drive current. Their disadvantage is that they are not expected to be commercially available until the 1980's. At this time, their price is not known.

Thyristors are not used because of the disadvantages mentioned. Field effect transistors seem to have the advantage but they are an advanced state-of-the-art technology and should not be considered at this time. At the present time, transistors are the best option.

SUSPENSION SYSTEM

The suspension system must have adequate flexibility to allow the rotor to rotate about its center of gravity without excessive bearing loading. It must not exhibit whirl vibration within the operating range. Also, bearing losses must be minimized.

The flexibility of the system is provided by mounting each bearing housing on a rubber pad. Extra damping is added into the system by the lower damping pad. Since it carries no thrust load, this pad can be quite soft, allowing it to add damping to the system. The system is shown schematically in Figure 24.

The dynamic properties of the system were analyzed and the results are plotted in Figure 25. It can be seen that no whirl vibration occurs within the operating range of 4,900 rpm to 9,800 rpm.

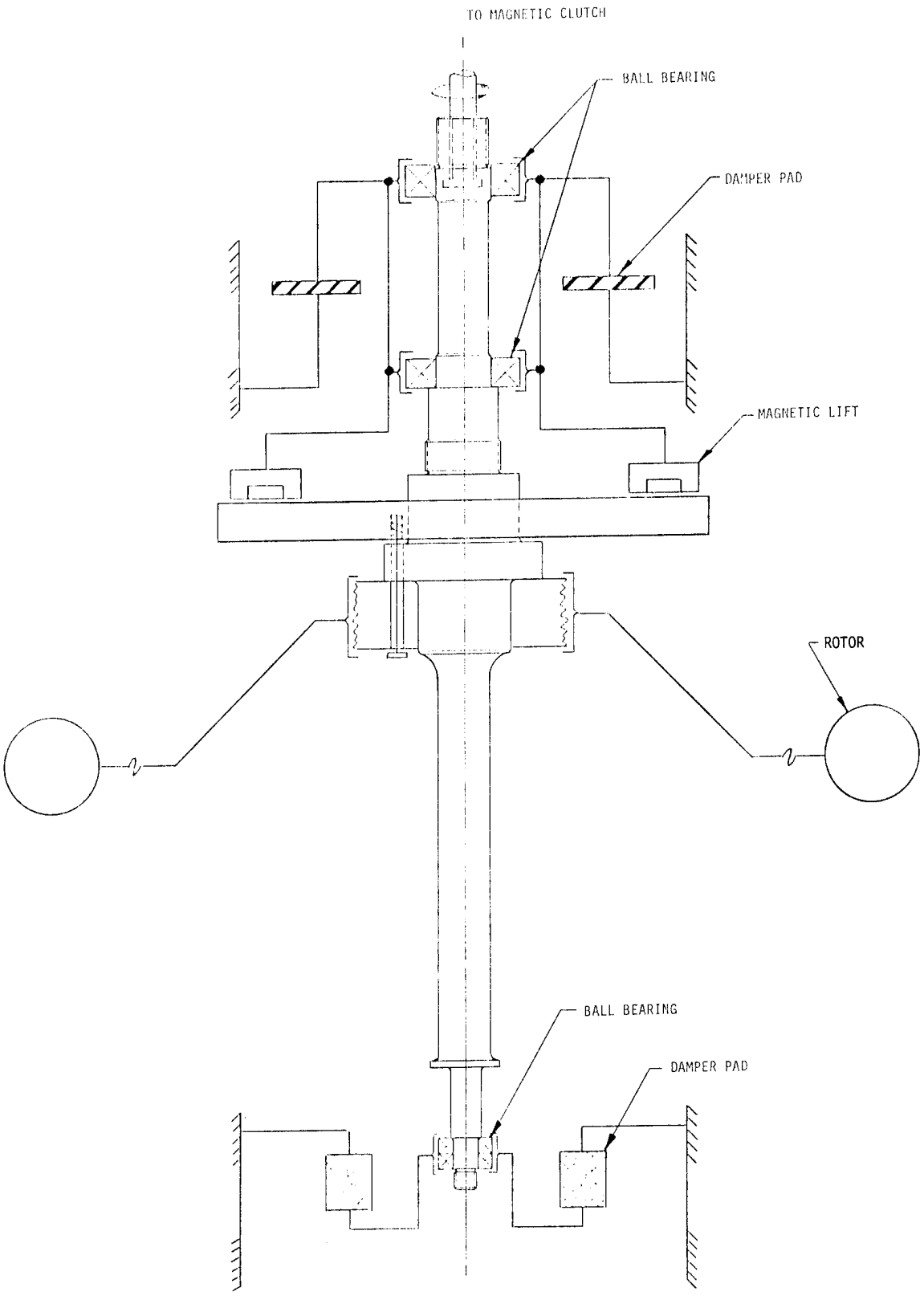

Figure 24. FESS Suspension Geometry

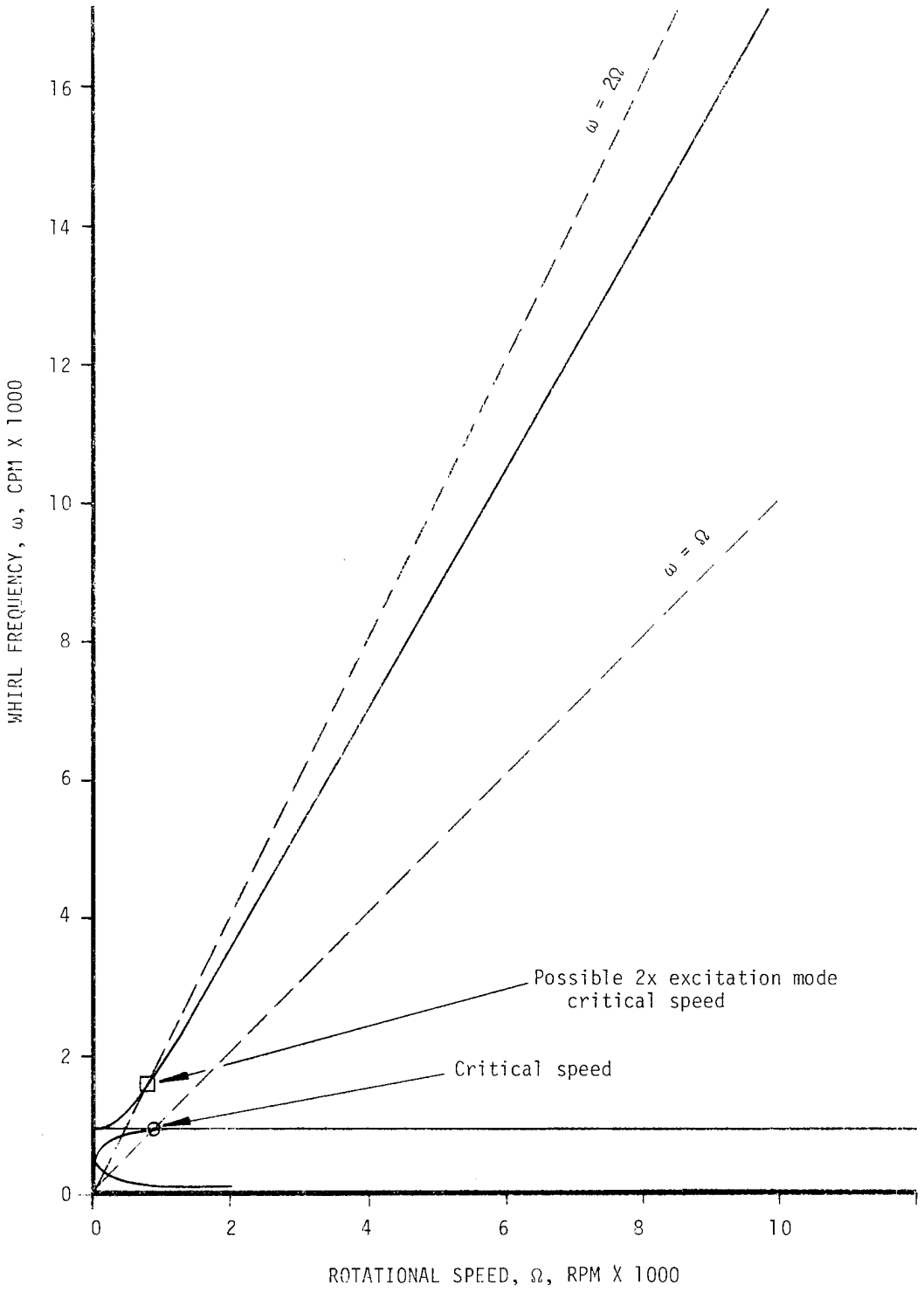

Figure 25. FESS Whirl Frequency vs. Rotational Speed

Three bearing configurations were considered:

All ball bearing

All magnetic bearing

Ball bearings combined with magnetic bearings

The all ball bearing configuration was not used because the high thrust load (900 lbs) would cause the bearing lifetime to be quite short. Also, the losses would be high.

All magnetic bearings were not used because they require very complex circuitry to keep them stable.

Ball bearings were used for radial stability and magnetic bearings were used to provide 90 percent of the thrust load. This configuration gives the longest bearing life and the lowest bearing losses.

SYSTEM OPTIMIZATION

EFFICIENCY

Run-down losses at 10,000 rpm are listed in Table 10. Total losses are 150 watts which correspond to 1.5 percent per hour. The pie graph in Figure 26 illustrates the relative magnitude of the run-down losses.

Run-down losses vary with speed. A graph of losses vs. speed is shown in Figure 27.

A major factor in run-down losses is windage. In order to minimize this, the enclosure is evacuated. A graph of windage as a function of vacuum level is shown in Figure 28.

Power conversion losses are listed in Table 11. The motor losses are illustrated in a pie graph in Figure 29.

Power conversion efficiency is a function of power level and speed. A graph of the round trip (charge and discharge) efficiency as a function of speed at two power levels is shown in Figure 30. At the maximum power level of 5 kW, the average efficiency over the operating range is an essentially constant 71 percent. This value drops with decreasing power levels in the manner shown in Figure 30.

Solar insolation data was provided by Sandia for two representative sites: Albuquerque, New Mexico, and Blue Hill, Massachusetts. This data is summarized in Table 12.

TABLE 10. Run-Down Losses at 10,000 rpm for 10 kWh FESS

COMPONENT	LOSSES IN WATTS
Main Bearings	36
Bottom Damper Bearings	2
Magnetic Coupling Bearings	23
Magnetic Lift Excitation	30
Magnetic Lift Hysteresis	4
Magnetic Lift Eddy Current	20
Oil Lube Pump	2
Windage	33
TOTAL	150

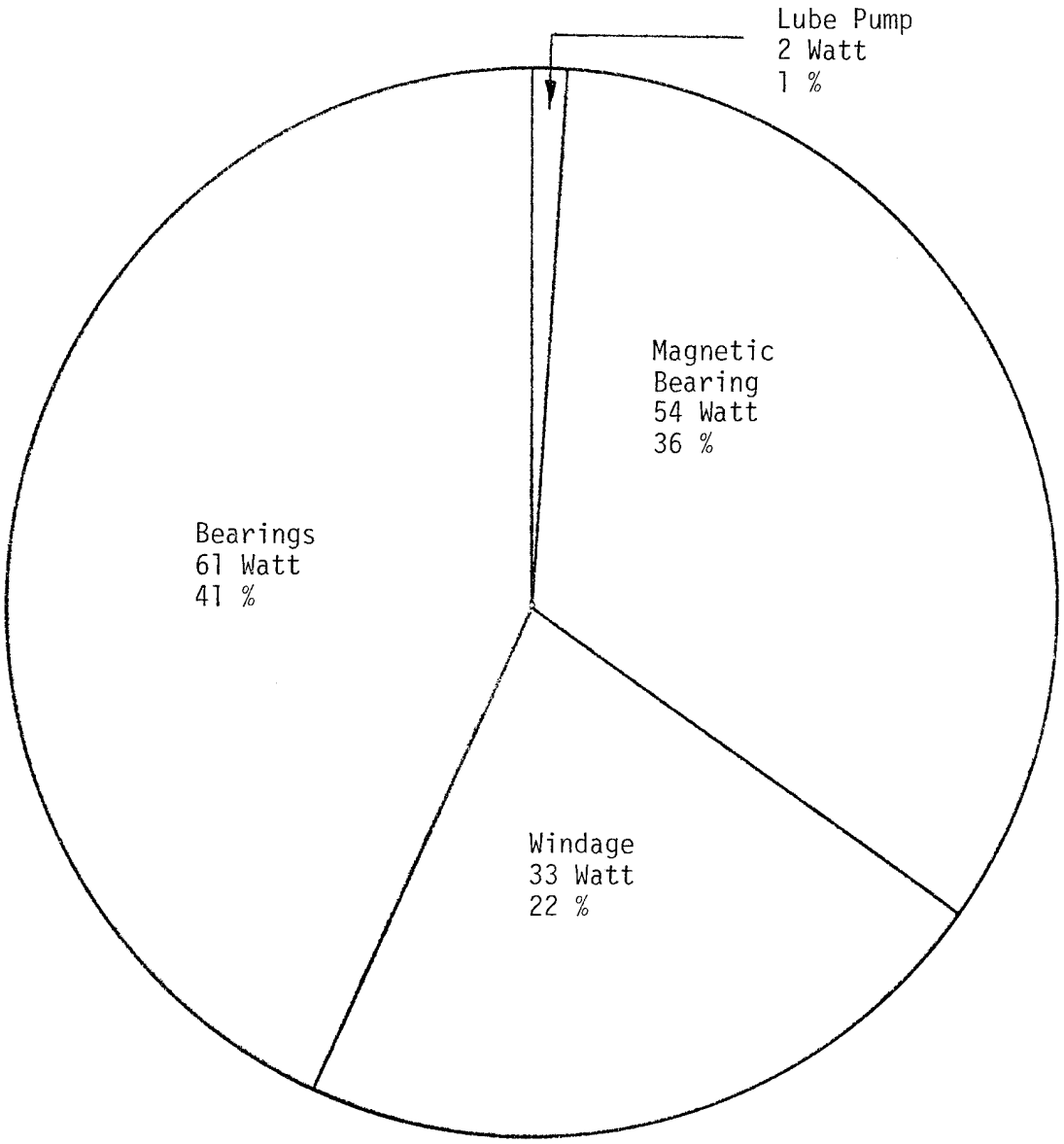

10,000 rpm - No Load

Figure 26. Run-Down Loss Chart

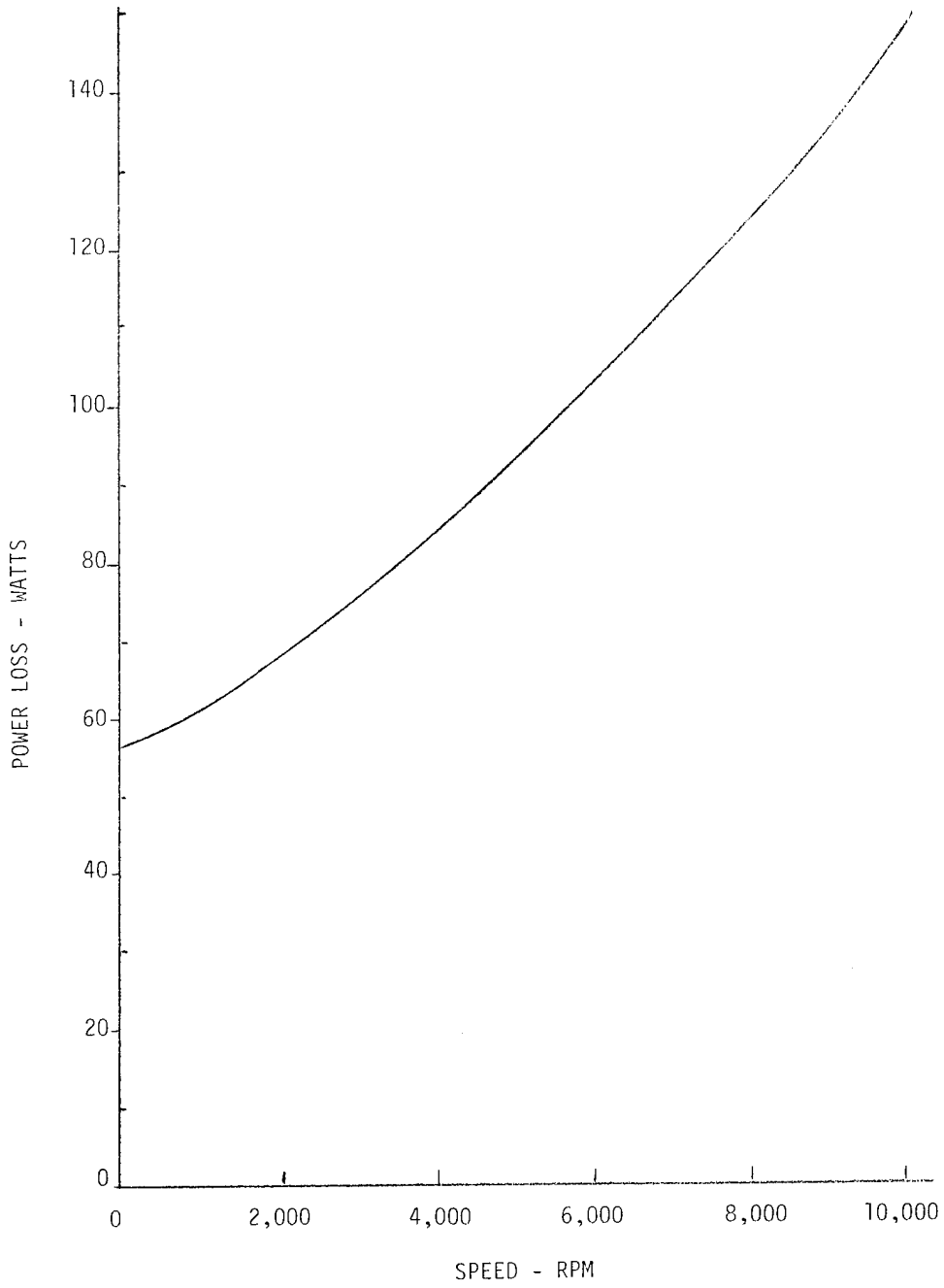

Figure 27. Run-Down Loss vs. Speed

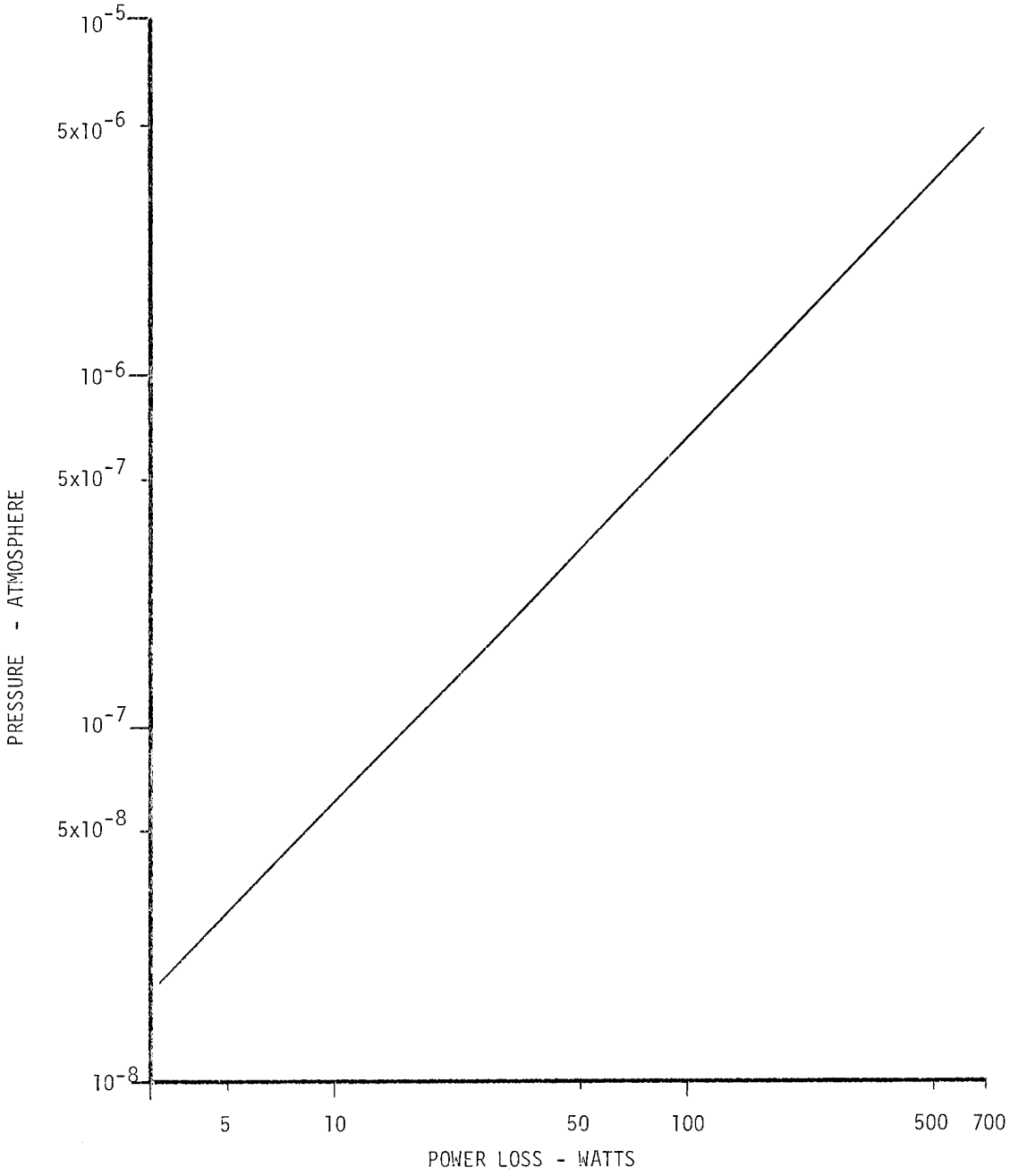

Figure 28. Power Loss vs. Vacuum Level

TABLE 11. Power Conversion Losses, 10-kWh FESS @ 9,800 rpm, 5-kW Motor

COMPONENT	LOSS IN WATTS
Magnetic Coupling	112
Stator	145
Core	12.5
Windage	80
Bearings	8
Slip Ring, Mechanical	50
Slip Ring, Voltage Drop	25
Field	32
TOTAL	464.5

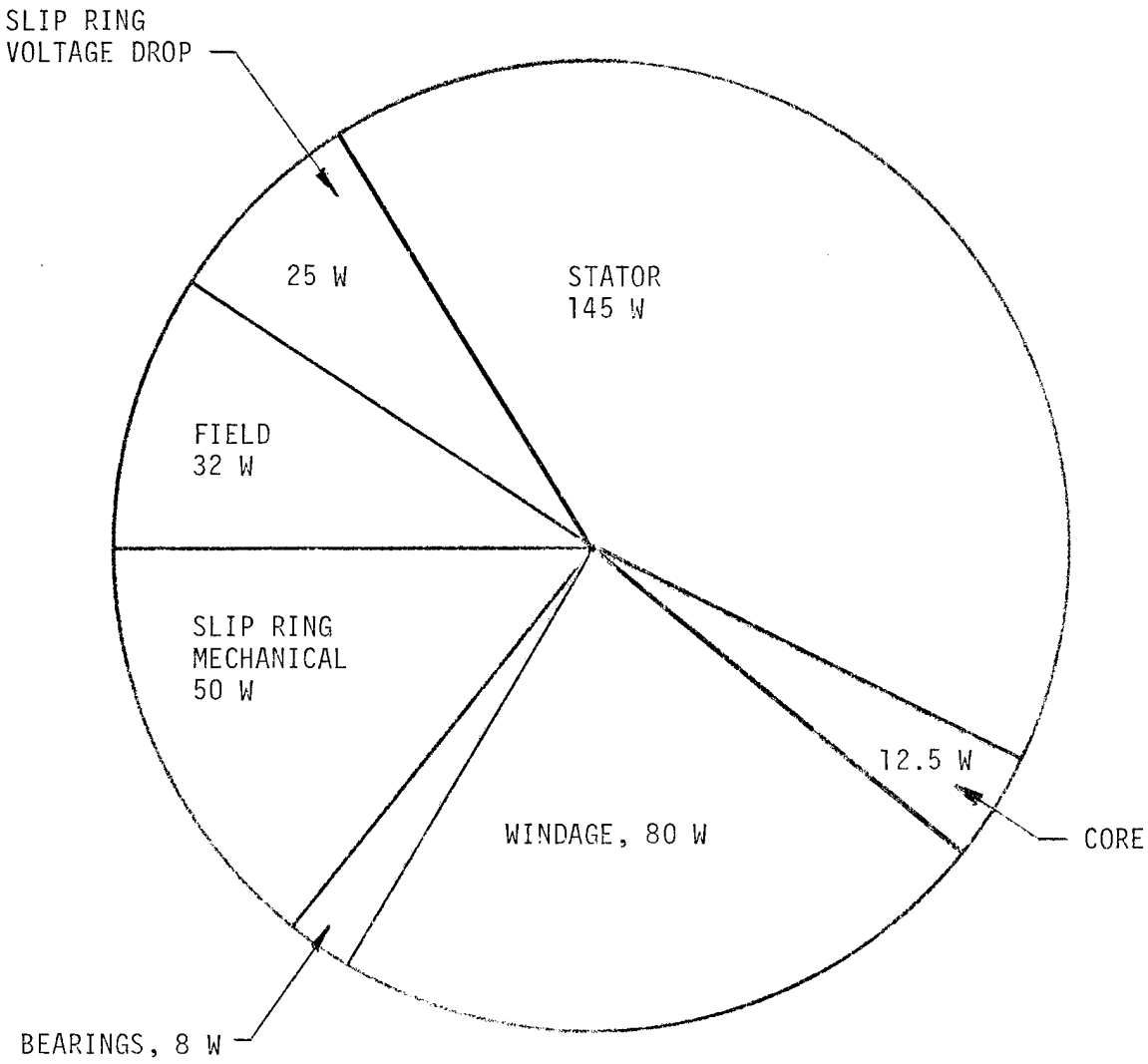

Figure 29. 5-kW Motor Losses @ 9,800 rpm

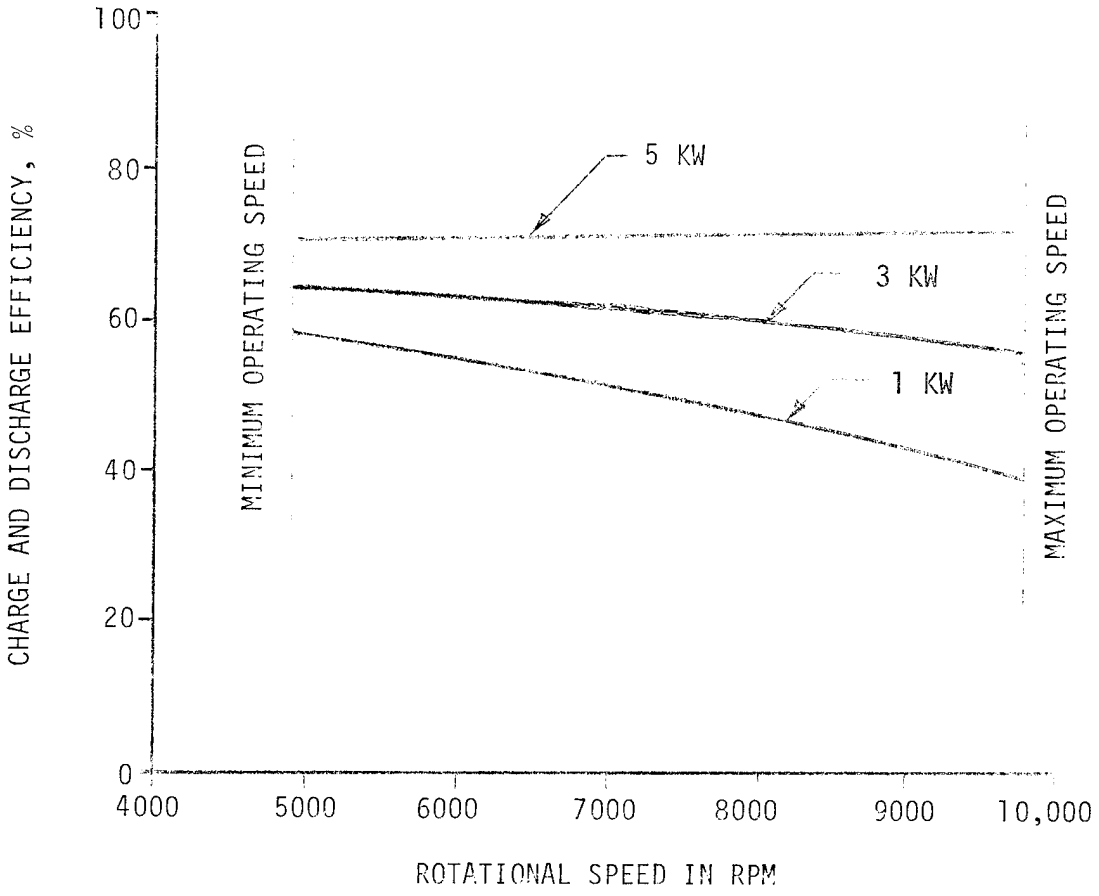

Figure 30. Charge/Discharge Efficiency

TABLE 12. Solar Insolation Data Summary

	ALBUQUERQUE	BLUE HILL
PEAK POWER TO FESS	7.52 KW	6.94 KW
PEAK ENERGY AVAILABLE FOR STORAGE	42.48 KWH	39.23 KWH
PEAK SEASONAL AVERAGE AVAILABLE FOR ENERGY STORAGE	38.70 KWH/DAY	29.58 KWH/DAY
PEAK SEASONAL RMS AVAILABLE FOR ENERGY STORAGE	38.82 KWH/DAY	39.98 KWH/DAY
YEARLY AVERAGE ENERGY AVAILABLE FOR ENERGY STORAGE	26.50 KWH/DAY	20.88 KWH/DAY

This Sandia-supplied data was analyzed to establish the relationship between the storage capacity of the FESS and the percentage of time (i.e., days of the year) that a particular capacity would accommodate all of the PV-supply output that was in excess of the residential load demand. The results of this analysis are shown graphically in Figure 31.

RELIABILITY AND SAFETY

The overall design life of the system is 20 years. Certain parts such as the rolling bearings and the slip ring brushes were designed for periodic replacement. Stresses in rotating parts were kept as low as possible to ensure reliable operation. As the mechanical system is hermetically sealed, it is anticipated that reliability similar to that of hermetically sealed refrigeration units can be achieved. High-reliability industrial-grade electronic components were called out to ensure a 20-year lifetime with minimum service requirements.

The safety hazard in the event of total failure of the wheel and vacuum vessel is eliminated by installation of the unit in a pit. The pit which provides environmental isolation and noise isolation also provides for rotor failure. Electrical wiring placed in conduit in accordance with local building codes is not expected to provide any safety hazards as the voltages and currents involved are similar to those found in present house wiring systems. Special effort should be taken, however, to ensure that insulation on wiring on the dc bus from the solar panels remains intact. This dc bus is considerably more dangerous than the ac voltages found in present house wiring.

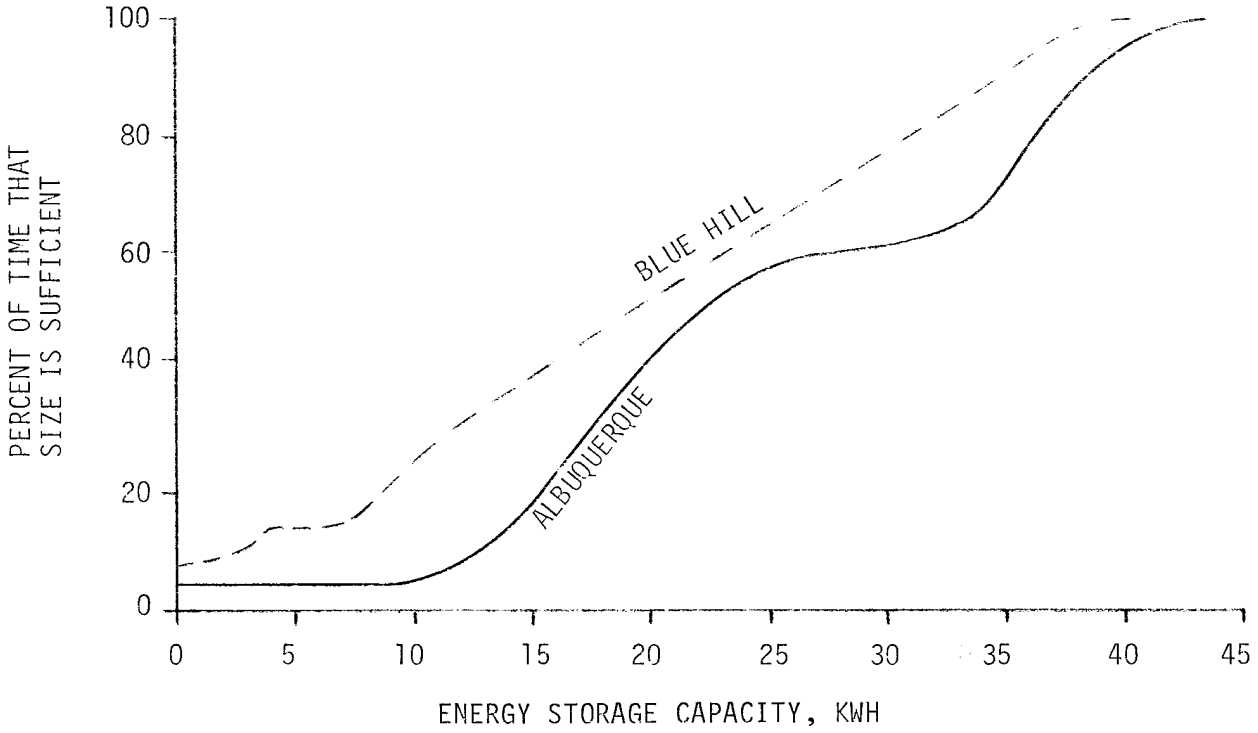

Figure 31. Adequacy of Energy Storage Capacity

FIFTY-KWH FLYWHEEL ENERGY STORAGE SYSTEM

CONCEPTUAL DESIGN

The preliminary design of the 50-kWh FESS is shown in Figures 32, 33, 34, and 35. The rotor assembly, proper, was scaled by a factor of 50/10 for all components in weight and a factor of $\sqrt[3]{5}$ in all dimensions. The magnetic coupling size is increased due to the higher torque required by the higher power rating and the lower speed.

COST ESTIMATE

In estimating the cost of the 50-kWh, 10-kW FESS, heavy dependence was placed upon the methods and unit costs developed for the 10-kWh storage system. Because of the greater weight of materials in the larger unit, break points in material cost occur for a smaller number of units.

Table 13 gives the estimated 50-kWh mechanical assembly cost. Table 14 gives the estimated 50-kWh total system cost including the mechanical assembly, the electrical controller assembly and the synchronous inverter. In production quantities of 100,000 units per year, the estimated total system cost is $18,561 (1979 dollars). This amounts to a $371 initial capital cost per usable kilowatt-hour stored for the 20-year lifetime unit.

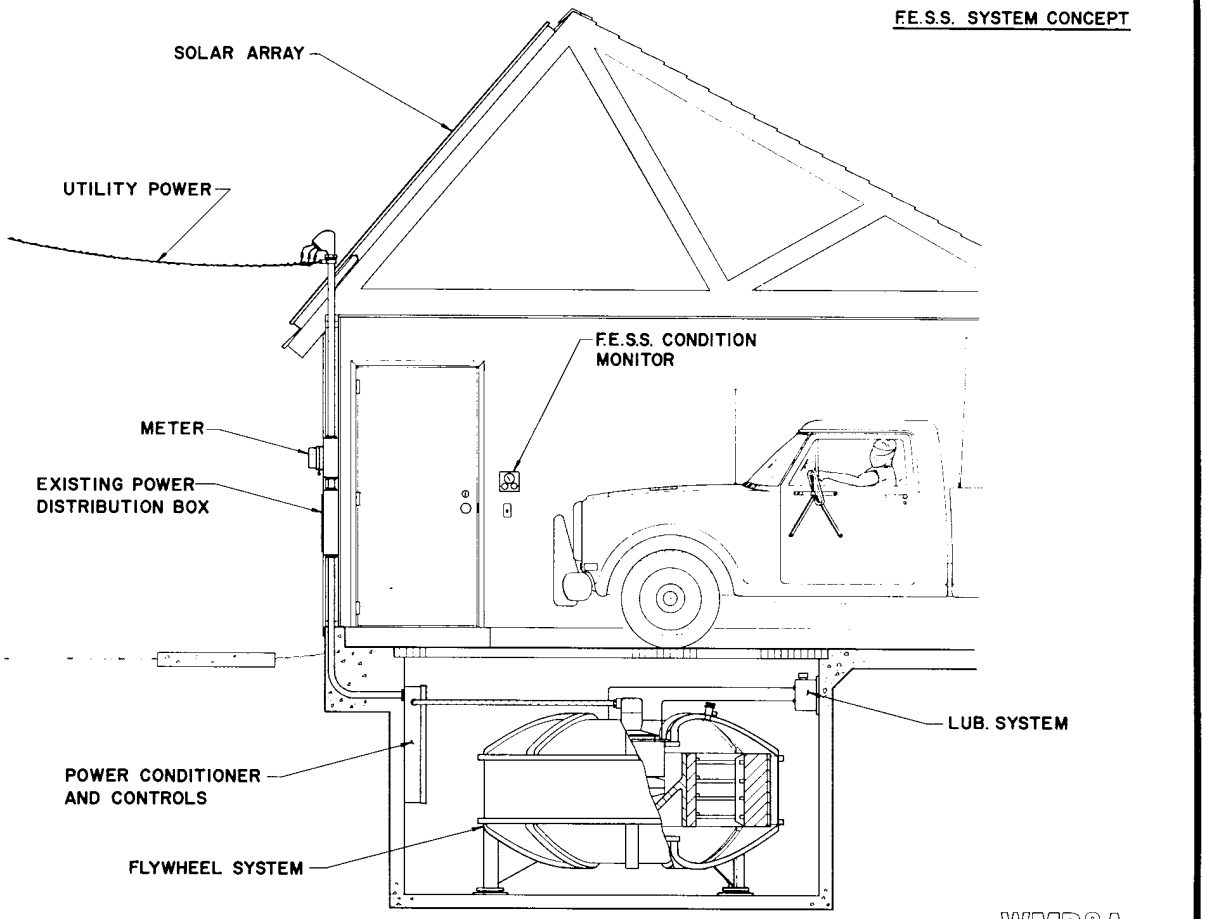

Figure 32. Fifty-kWh System Concept

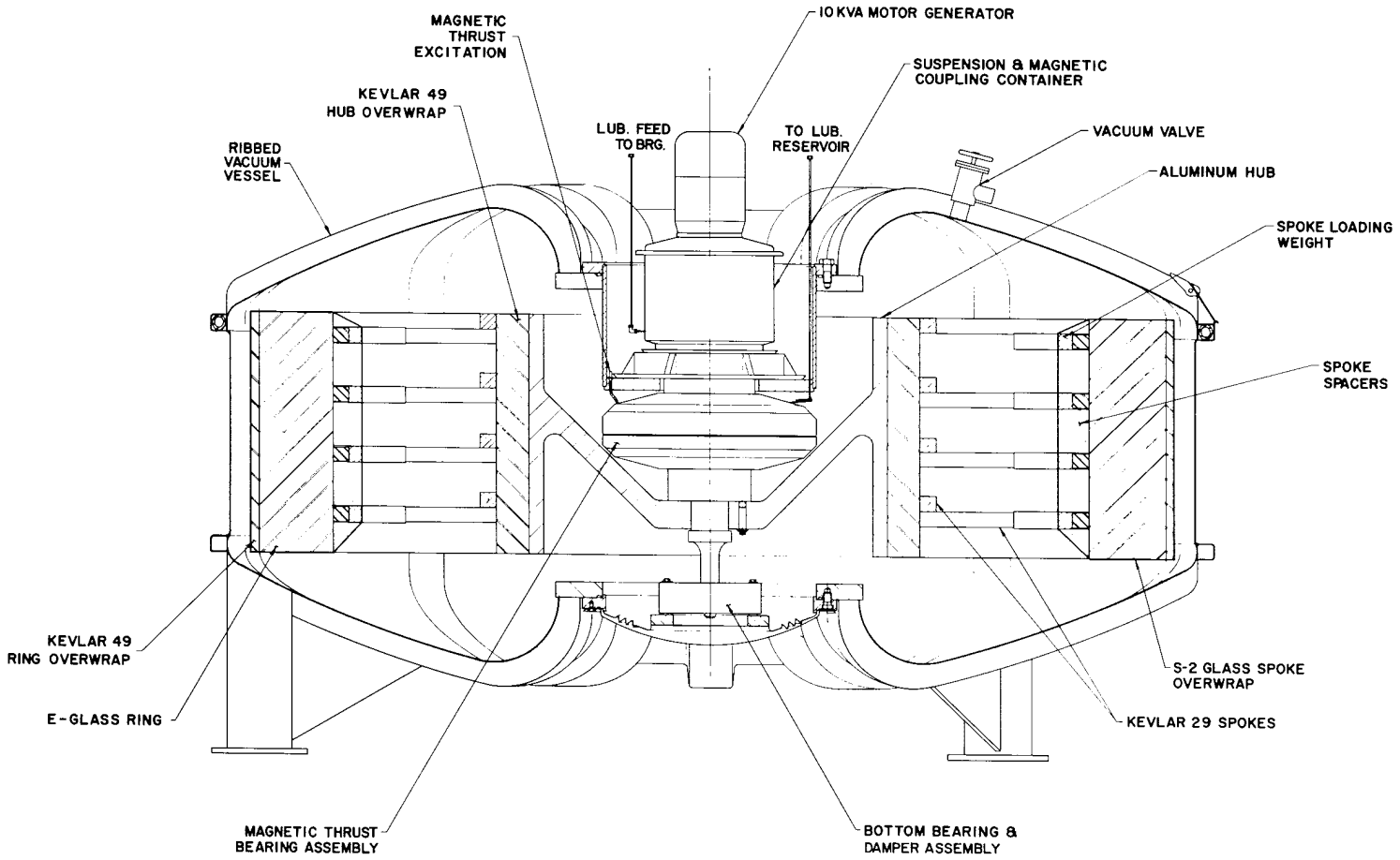

Figure 33. Fifty-kWh FESS

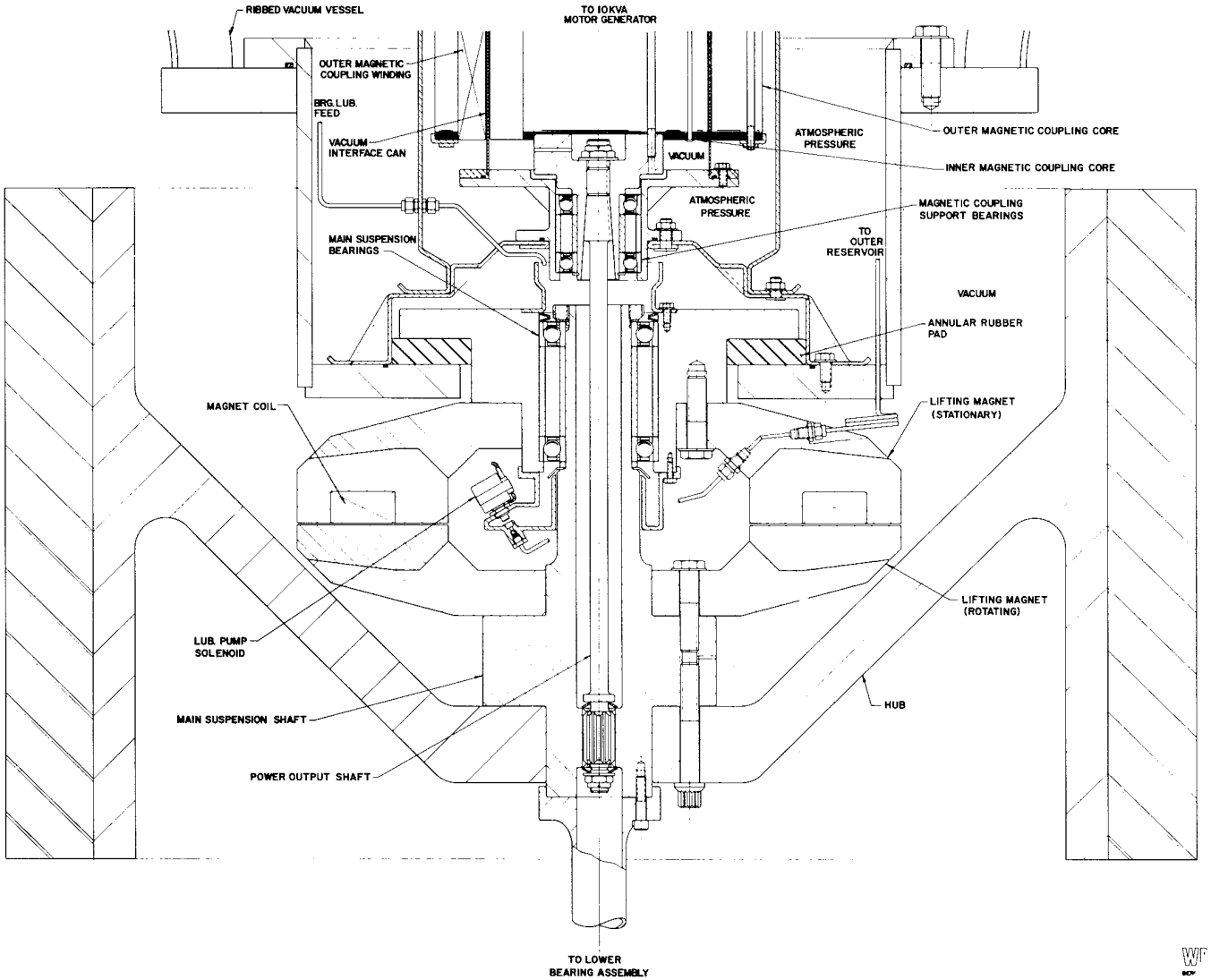

Figure 34. Fifty-kWh Suspension and Magnetic Coupling

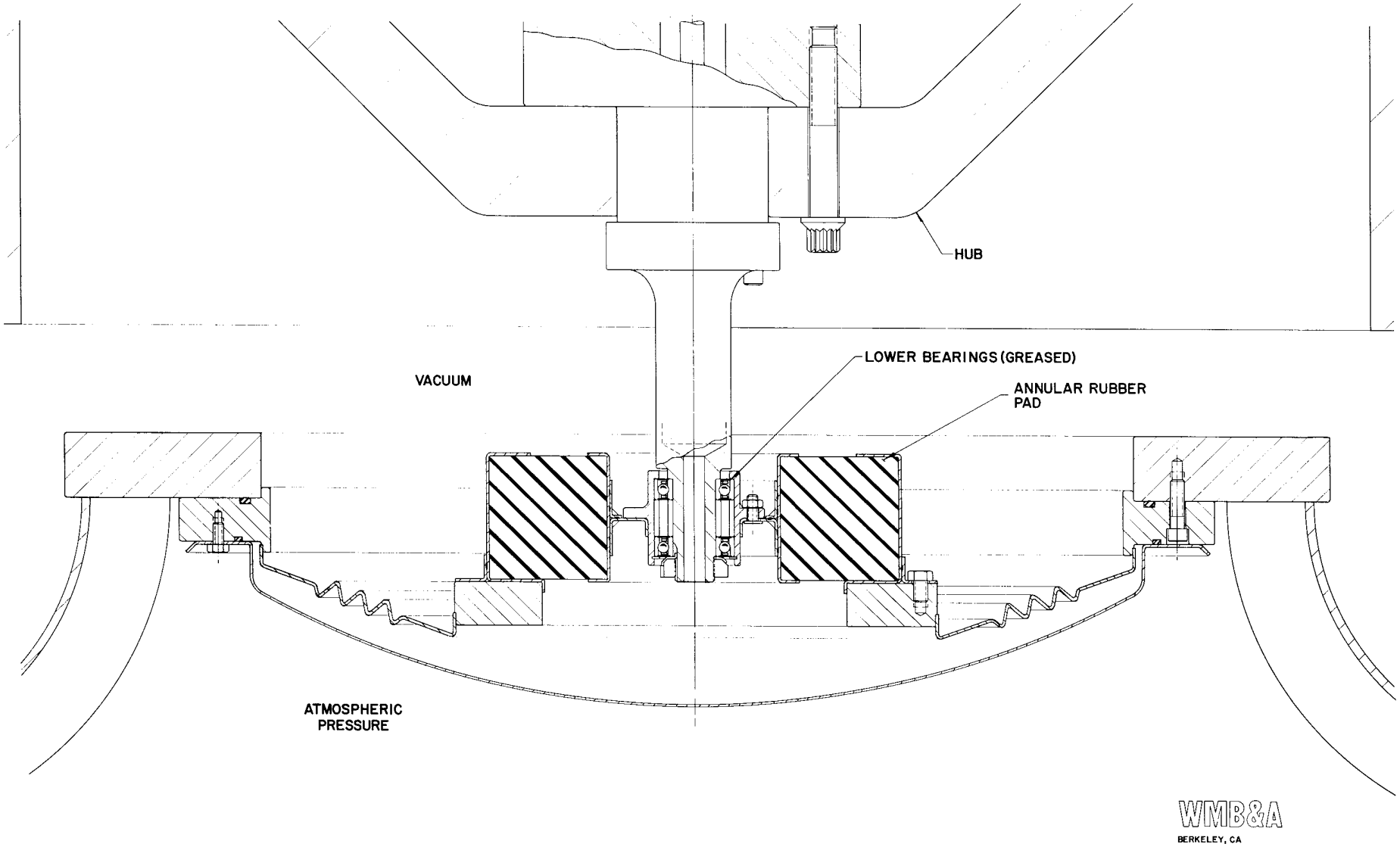

Figure 35. Fifty-kWh FESS Lower Suspension

Table 13. Cost Per Assembly - 50-kWh, 10-kW FESS Mechanical Assembly

NO. OF ASSEMBLIES	FABRICATED COMPOSITES COST $	ASSEMBLED ROTOR COST $	COMPONENT CATEGORY[1] (a) COST $	(b) COST $	(c) COST $	(d) COST $	TOTAL COMPONENTS COST $	MISC. HDWE COST[2] $	MAGNETIC COUPLING COST $	ALTERNATOR COST $	TOTAL PARTS COST $	ASSEMBLY LABOR COST[3] $	TOTAL COST PER ASSEMBLY[4][5] $
10^2	15754	18230	200	905	1467	195	2767	452	544	1514	23510	2350	25860
10^3	14116	16190	177	770	1313	166	2426	418	462	1287	20783	1558	22340
10^4	12825	14620	150	654	1202	141	2147	372	393	1094	18626	934	19560
10^5	11846	13400	128	556	1138	120	1942	246	334	930	16850	845	17695

[1] a. Heat treated ground steel components; b. carbon steel ground components; c. formed sheet steel components; d. machined fabrications.

[2] Ten percent of total components cost + estimated bearing cost.

[3] Ten percent, 7.5 percent, 5 percent, 5 percent of total parts cost, respectively.

[4] Does not include development nor tooling costs.

[5] 1979 dollars

TABLE 14. Cost Estimate for 50-kWh FESS
(1979 Dollars)

QUANTITY	MECHANICAL	CONTROLLER	INVERTER	TOTAL
10^2	25,860	706	1589	28,155
10^3	22,340	623	*485	23,448
10^4	19,560	564	411	20,535
10^5	17,695	516	350	18,561

* Represents the change from a commercially purchased unit to an in-house design.

TEN-KWH DEMONSTRATION FESS

DESIGN DESCRIPTION

Layout drawings, specifications and cost estimates for a prototype 10-kWh, 5-kW FESS have been prepared based upon the concept previously presented. The prototype FESS is assumed to be a one-off, hand-built demonstration system. The system cross-section is shown in Figure 36. This unit differs from the production model primarily in terms of its fabrication requirements. It is designed to be fabricated with a minimum of special tooling. The vaccum vessel is a welded structure not necessarily suitable for high-quantity production. A comparison of Figures 36 and 4 reveals the significant differences between a production FESS and a prototype FESS.

COST ESTIMATE

The cost estimate for fabrication of one prototype demonstration unit includes cost not accounted for in the high quantity production estimates. The costs include items like tooling, assembly fixtures, casting molds and multiple tries, etc. In one-off quantities, these costs dominate the cost of the system. It should also be emphasized that the actual design of the prototype unit is different from that of the production unit. These differences reflect the differences in manufacturing techniques between high and low quantity production. The fixtures and tooling, etc., would be designed only for one-off production and their cost would have no bearing

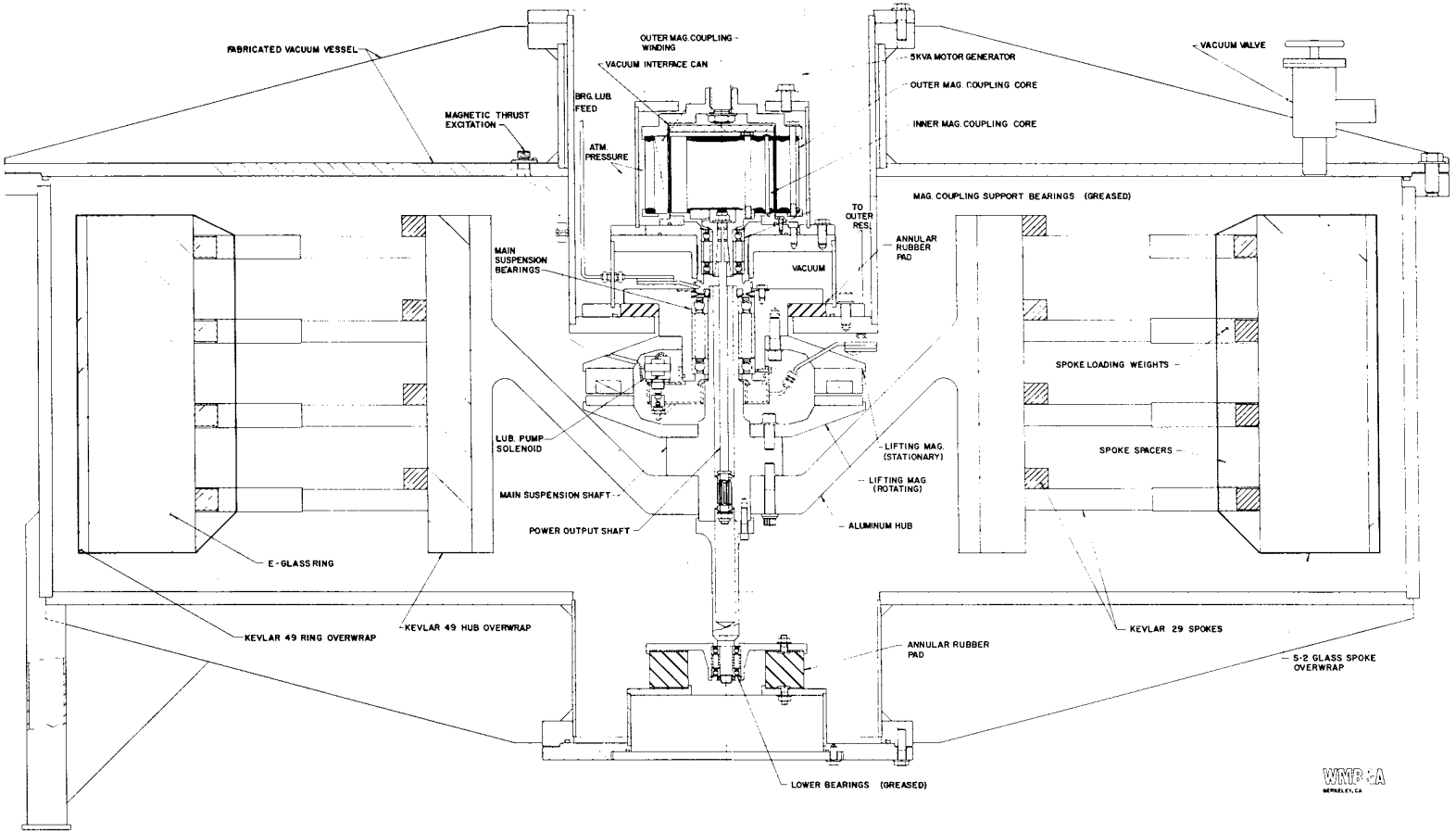

Figure 36. Ten-kWh FESS Demonstration System

on tooling costs for the high production units although it is expected that much information gained from a one-off fabrication would directly aid the high quantity unit.

Table 15 lists the estimated costs for producing one prototype 10-kWh flywheel energy storage system.

Additional costs including a testing program, administration costs and further design, etc., would have to be added to yield an actual delivered system cost.

TABLE 15. Cost Estimate for Prototype 10-kWh Demonstration FESS

1.1	Rotor-Hub-Spoke Assembly	$ 39,525
1.2	Suspension and Mag Coupling Assembly	22,275
1.3	Lower Suspension Assembly	2,190
1.4	Motor Generator Modified	4,350
1.5	Vacuum Vessel	6,108
1.6	Accessories	12,650
1.7	Final Assembly and Checkout	9,000
1.8	Tooling and Fixtures	59,600
	Mechanical Total	$155,698
2.1	Breadboard Assembly	$ 26,000
2.2	Prototype Assembly	23,465
2.3	Inverter	2,270
	Electrical Total	$ 51,735
	ESTIMATED TOTAL SYSTEM PRODUCTION COSTS FOR ONE 10-kWH PROTOTYPE UNIT	$207,433

CONCLUSIONS AND RECOMMENDATIONS

This design study indicates that a reliable, efficient flywheel energy storage system can be manufactured at a reasonable cost.

It is recommended that a prototype model be produced to demonstrate the viability of the concept.

REFERENCES

1. Younger, F. C., "Tension-Balanced Spokes for Fiber-Composite Flywheel Rims," 1977 Flywheel Technology Symposium, Conf-771053, March 1978.

2. Thomson, W. T., Younger, F. C., and Gordon, H. S., "Whirl Stability of the Pendulously Supported Flywheel System," Journal of Applied Mechanics, Vol. 44, Trans. ASME, Vol. 99E, June 1977, pp. 322-328.

3. Den Hartog, J. P., "Mechanical Vibrations," 4th Ed., McGraw-Hill Book Co., New York, NY, 1956.

4. "Aerospace Structural Metals Handbook," maintained by Mechanical Properties Data Center, Battelle-Columbus Laboratories, Columbus, Ohio.

5. Clements, L. L. and Moore, R. L., Lawrence Livermore Laboratory Report UCRL-79262 (1977).

6. Poehlmann, H. C., "Outgassing Tests of Fiber/Epoxy Composite Materials," Sandia Laboratories, Report No. SAND78-7075, February 1979.

7. Markley, F., Roman, R., and Vosecek, R., "Outgassing Data For Several Epoxy Resins and Rubbers for the Zero Gradient Synchrotron," 1961 Transactions of the Eighth Vacuum Symposium and Second International Congress, Pergamon Press, 3rd Ed., 1962.

8. Timoshenko, S., "Strength of Materials," Part II, D. Van Nostrand, Princeton, NJ, 1956.

DISTRIBUTION:

DOE/TIC-4500-R67 UC-94b (183)

William M. Brobeck & Associates (5)
1235 Tenth St.
Berkeley, CA 94710

University of California (2)
Lawrence Livermore Laboratory
P. O. Box 808
Livermore, CA 94550
Attn: T. M. Barlow MS L-388
D. M. King ML L-388

SERI (2)
1536 Cole Blvd., Bldg. #4
Golden, CO 80401
Attn: Library

ARRADCOM
Plastics Technical Evaluation Center
Dover, NJ 07801
Attn: A. M. Anzalone, Bldg. 3401

US Department of Energy (2)
Albuquerque Operations Office
P. O. Box 5400
Albuquerque, NM 87185
Attn: D. K. Nowlin, Director
Special Programs Division

US Department of Energy (2)
Division of Energy Storage Systems
600 East St. NW
Washington, DC 20585
Attn: J. H. Swisher
P. Thompson

US Department of Energy (2)
Division of Distributed Solar Technology
600 East St. NW
Washington, D. C. 20585
Attn: R. L. San Martin
P. D. Maycock

2320 K. L. Gillespie
2324 R. S. Pinkham
2324 H. E. Schildknecht
4715 R. H. Braasch
4719 D. G. Schueler
4740 R. K. Traeger
4742 A. F. Veneruso
4744 H. M. Dodd
4744 B. C. Caskey
5811 L. A. Harrah
5844 F. P. Gerstle
8266 E. A. Aas
3144 T. L. Werner (5)
3151 W. L. Garner (3)
For DOE/TIC (Unlimited Release)

Org.	Bldg.	Name	Rec'd by *	Org.	Bldg.	Name	Rec'd by *

* Recipient must initial on classified documents.